THE SINTERING OF METALLIC POWDERS

T H E S I S

submitted to the

UNIVERSITY OF GLASGOW

for the

Degree of Doctor of Philosophy

by

JAMES BRUCE MARRIOTT, B.Sc., A.R.T.C.

September, 1955.

C O N T E N T S.

CHAPTER I.

INTRODUCTION.

INTRODUCTION.

The term sintering can be defined as the process whereby bonds are formed between adjacent particles in a powder and subsequently the voids between those particles gradually isolated and eliminated, all in the absence of a liquid phase. In order to avoid confusion in discussion of this subject the term sintering will be applied exclusively to the treatment of unimetallic powders. For the treatment of multi-metallic powders the term alloy-sintering will be used.

A very considerable amount of research has been, and is being directed towards increasing our knowledge of these two processes, as can be judged from the large number of publications dealing with the subject.

Most of the work has had as an object the establishment of the mechanism of sintering, and as a result a number of mechanisms have been proposed. Fewer papers, however, have dealt with alloy-sintering, particularly of mixtures of metals which are known to form stable compounds.

Alloy sintering is a more complex process as in addition to the process of sintering already defined complicating factors arise, such as the osmotic pressure caused by unequal rates of diffusion of the two components and the possibility of the formation of intermetallic compounds. Both of these tend to disrupt the compacted powder, so opposing the progress of densification.

The present investigation has been confined to the study of this type of process. The progress of alloy-sintering in binary systems, where intermetallic compounds are known to form, has been investigated in order to study the initiation and progress of intermetallic compound formation in the compacts. The progress of homogenisation after the initial compound formation has also been studied.

To carry this out the following experimental methods have been used:-

(a) Differential thermal analysis of compacted powders,

(b) Thermal evaporation in vacuum of a metal and its deposition on a powder compact of another metal.

(c) X-ray analysis by powder techniques of partially sintered compacts and specimens prepared as in (b).

CHAPTER II.

REVIEW OF THE LITERATURE.

REVIEW OF THE LITERATURE.

During the sintering of a metallic powder there must be a considerable amount of atomic movement and re-arrangement to effect the bridging, isolation and final elimination of the voids which are initially present.

A number of theories have been propounded to explain the mechanism of sintering. Some refer to sintering which takes place in the presence of inter-connected pores. This condition is found in the earlier stages of sintering. Others refer to sintering when the pores are closed, as happens during the later stages.

Since in this investigation we are concerned with changes occurring at an early stage in the sintering process, it would seem sufficient to mention briefly some of the theories put forward to account for the earlier stages of sintering. The theoretical and experimental data on all stages of sintering have been fully reviewed by Roberts(1) and Goetzel(2).

The theories referring to sintering while the pores are inter-connected can be divided into two classes, those which favour a diffusional mechanism and those which favour flow under the action of surface tension forces. In many cases it has been shown that the radius of the interface (x) between two particles is related to the time of sintering (t) by an equation of the type $x^n = At$.

Diffusional Type.

Evaporation-Condensation.

According to this theory material is transferred from one surface to another, over which the vapour pressure of the material is lower. Since a more curved surface would have a lower vapour pressure, material should be deposited on the parts of a pore with the smallest radius. However, Roberts(1), among others, has shown that the rate of metal transfer is such that any sintering by this means is negligible.

Volume Diffusion.

Kuczynski(3) considered a possible mechanism where surface forces, which tend to decrease the total surface area, would tend to build up a high concentration of vacant lattice sites in the material near the contact area between two particles, or as was the case in Kuczynski's experiments, between a particle and a plane surface. The vacant lattice sites would then diffuse away, resulting in a net flow of material into the area of contact. In this type of mechanism the rate of sintering would be such that

$$n = 5; \text{ i.e., } x^5 = At.$$

Kuczynski measured the rate of increase of contact area between a sphere and a plate for copper and silver. Since these experiments showed that n = 5 (approximately) he concluded that volume diffusion

was dominant. Confirmation was provided by the fact that the activation energy for volume diffusion calculated from this data agreed well with that calculated for self diffusion by tracer techniques.

Surface Diffusion.

During his investigation Kuczynski found that when sintering small particles (less than 30 microns) n = 7. This could be explained, he suggested, by assuming surface diffusion to be operative. Subsequently Cabrera(4) gave a more precise treatment for the volume and surface diffusion mechanisms in the sphere-on-plane experiments. In the case of volume diffusion, he obtained a different value for the constant term than did Kuczynski. Otherwise, however, the equations were similar. On the other hand, when he considered surface diffusion, Cabrera derived a relationship in which n = 5, not 7 as Kuczynski had suggested. Thus, though it seemed probable that the larger spheres sintered by a volume diffusion mechanism, the mechanism involved in sintering the smaller spheres was known with less certainty.

More recently Arthur(5) has investigated porosity changes during sintering of copper powder, two ranges being used, 47-66 microns and -45 microns. On account of the existence of pores connected to the surface of the compact during most of the sintering period, he has suggested that surface diffusion may be operative.

Viscous and Plastic Flow.

Frankel(6) suggested that crystalline bodies would show a Newtonian viscosity at high temperatures. In a mechanism of this type the relation $x^2 = At$. would hold. He assumed that the particles would remain spherical, there being a line contact between them. Clark and White(7) studied the theory of both viscous and plastic flow. They likewise assumed that the particles would remain spherical, but that material would flow under the action of surface tension forces to form a lens between the particles. They also assumed that the flow would be confined essentially to the surface layers of the particles.

They found that a soda-lime glass sintered with a Newtonian viscosity, while both alumina and magnesia sintered according to the Bingham law.

From the foregoing it can be seen that volume diffusion is definitely operative under certain conditions, but that the case for surface diffusion is more uncertain. Plastic flow under the action of surface tension forces has been shown to be possible but viscous flow has only been observed in glasses. It would seem possible, therefore, that a diffusion mechanism of some type may be operative at least in the very early stages of sintering.

Alloy Sintering.

In the introduction it was suggested that the mechanism of sintering in a compact containing two metals would be more complex than that just discussed. This has in fact been shown to be the case. Differing rates of interdiffusion of the two metals and intermetallic compound formation are both found in certain circumstances and take place in reactions unrelated to the actual sintering process. They may, indeed, oppose the progress of sintering by causing further or larger voids to appear.

Interdiffusion.

The marker method of Smigelskas and Kirkendall(8) has proved to be of great value in studying the inter-diffusion occurring at the interface between two dissimilar metals. The method has been refined and improved by da Silva and Mehl(9) who found that in the alloys which they studied, almost any unreactive substance could be used as a marker. They gave as examples, metals, such as molybdenum and platinum, oxides, like alumina and iron oxide, and carbon. Three possible methods of using these markers were given.

In the direct method the distance between two sets of wires in a sandwich A-B-A is measured. This, however, does not take account of creep, internal gas reactions and other such factors. The accuracy can be improved, the authors say, if an impermeable foil is placed at the edge of the interface. Then the movement of the wire markers can be referred to this as a standard, so giving a measurement, unaffected

by these secondary factors. It has also been observed that when diffusion occurs round a foil, the edge bends progressively while the centre remains fixed. This bending also provides an accurate indication of the movement taking place.

The movement of the marker is always toward the block richer in the faster diffusing metal. It has also been observed that the amount of movement measured in a given system is independent of the material used for the marker. From their experiments da Silva and Mehl suggest that diffusion through vacant lattice sites is most likely and since the amount of shift is independent of the size of specimen, they conclude that the vacancies must be generated in the diffusion zone on one side of the interface and later condensed on the other side. They found little porosity in their specimens.

While investigating interdiffusion in the copper-nickel system Barnes(10) found that there was an increase in the volume of the diffusion zone as well as movement of the markers towards the area rich in copper, the faster diffusing metal. Microscopic voids were seen on the copper side of the interface which he explained by suggesting that there was a flow of vacancies in the reverse direction to the flow of atoms. Only some of these vacancies were destroyed, the remainder coalescing to form voids. In this way there could be a movement of the interface and yet an increase in volume.

Balluffi(11) referring to his own work while discussing the paper by de Hills and Nehl, stated that there are five possible mechanisms by which vacancies can condense. (a) they can diffuse to the surface, (b) they can condense on dislocations with a Taylor-Orowan characteristic (within the crystal or at the grain boundaries), or (c) on impurities of a macroscopic or even atomic nature, (d) they can condense to form voids initially probably plate like in form which soon collapse producing a dislocation ring, or (e) do voids which are probably roughly spherical in shape and do not collapse. If the vacancies condense by methods (a), (b) or (d), no voids will appear; if they condense by mechanisms (c) or (e), then, small voids may grow. The presence of gas in the metal would help to stabilize the voids once they had been formed.

Using specimens compacted from mixtures of copper and nickel powders, Butler and Hoare(12) observed an expansion of 6/7% during sintering. They found that in the compacts examined there were regions of high porosity on the copper side of the interfaces between grains and suggested that this porosity was due to the unequal rates of diffusion of the two metals. They also concluded that this interdiffusion was unrelated to sintering, and actually hindered it. The main driving force for sintering was said to be surface tension which caused plastic flow to occur.

It would appear from these investigations that there is no basic difference between the behaviour of diffusion couples and compacted mixtures of different metal powders. The main factors are

the increase in interfacial contact in a powder compact and the much shorter distances to be covered before homogenisation is achieved.

Intermetallic Compound Formation.

If, at a comparatively low temperature a bi-metallic compact undergoes a reaction in which some grains expand, they might be expected to do so by moving apart, rather than by deforming, thus increasing the proportion of voids present and causing the compact as a whole to expand. For this reason, possibly, the dilatometric technique has been much favoured for the study of sintering in systems containing intermediate phases.

Dilatometric methods.

Raub and Plate(13) have made an extensive dilatometric investigation of many binary systems. They concluded that a reaction between the two metals, forming an intermediate phase, caused a marked break in the dilatometric curve. Wherever possible they correlated their results with the phase diagram of the respective system. In all cases where intermetallic compound formation was indicated by the phase diagram an abrupt change in the dilatometric curve was recorded. On the other hand no discontinuities were observed in the dilatometric curves of those compacts composed of two metals which were known not to form intermetallic compounds. In certain systems for which no phase diagrams existed, discontinuous changes were obtained which indicated in a qualitative manner the existence of intermediate phases in these systems.

Duwez and Jordan(14) have studied the sintering of copper-gold alloys. At high temperatures this system shows a continuous solid solution range, but at lower temperatures ordered lattices are formed at and around the compositions corresponding to CuAu and Cu_3Au. Most of their investigation was made with the aid of X-ray techniques and more will be said about their results in the section dealing with X-ray examination, but some dilatometry was included. They found a large expansion, reaching 14% at the composition of Cu_3AU, in a short temperature range, and after consideration of their X-ray results they concluded that it marked the formation of an intermetallic compound.

In addition, Duwez(15) has studied the sintering of compacts of copper and nickel, copper and zinc, and copper and tin. In the copper-nickel system where, no intermediate phases appear, a small steady expansion was obtained up to a certain temperature, after which shrinkage was observed. This was very similar to the behaviour of a unimetallic compact and indeed the curve for the alloy could be computed, approximately from those of the pure metals.

In the copper-zinc and copper-tin systems, on the other hand, discontinuous expansions occurred at low temperatures. Taking the copper-zinc system as an example, Duwez explained those results in the following manner. Since the solubility of copper in zinc is small and that of zinc in copper large, the zinc will diffuse into and dissolve in the copper and thus cause the copper to expand. Cavities will be left where there were grains of zinc, but as the plasticity of the copper

particles is low at these temperatures, they will retain their shape and expand by their centres moving apart rather than by deforming and so filling the voids. It was thought that when the zinc diffused into the copper an intermetallic compound might be formed.

It is interesting to recall the observations of Butler and Hoare who obtained a discontinuous expansion of about 6% in copper-nickel compacts, no expansion of this kind being observed in either of the pure metals. The total expansion obtained by Duwez for this system was about 1%. Duwez used a naturally graded powder, normally -300 mesh. Butler and Hoare, on the other hand, used a fairly uniformly sized powder of particle size about 4·5 microns. This and possible differences in compact preparation probably holds the key to the difference between Butler and Hoare's results and those of most other observers.

The sintering of copper-zinc compacts has been thoroughly investigated by Nevat, Creik and Cranston(16) using a number of methods. In their dilatometric studies they found that as the composition of the compact was varied from 5 to 50% Zn the total expansion increased. They also observed that increasing the size of the zinc powder from -300 to -120 mesh had little effect on the shape of the curve, while increasing the size of the copper powder by the same amount increased the discontinuous expansion considerably. Increasing the compacting pressure for a given mixture of powders caused the observed expansion to fall, due possibly to the increase in strength of the compact. However, with a compacting pressure of more than 30 tons/in^2, the expansion gradually

rose again. This, they suggested, could be due to increasing cold welding facilitating intermetallic compound formation. Throughout these different trials the temperature at which the sudden expansion occurred remained reasonably constant, though it rose slightly with increase in copper particle size.

The other methods used by Howat, Craik and Cranston included differential thermal analysis, electrical resistivity, and an X-ray study of the phase present at various stages of sintering. Some of these will be mentioned in the following sections.

Differential Thermal Analysis.

Using this method, Howat, Craik and Cranston, found that there was a sharp exothermic change at the same temperature as the discontinuous expansion in the dilatometric investigation. This change increased in magnitude from 10% to 50% Zn.

They concluded that quantities of an inter-metallic compound (the β phase) were formed initially in any compact within this range of composition. It was also noted that since the temperature of the exothermic change corresponded with that marking the beginning of the aprupt expansion in their dilatometric studies, this expansion must be due, partly to the initial formation of a copper-zinc compound.

Increasing the size of both the copper and the zinc particles led to a lessening in intensity and broadening of the change until it almost disappeared. At the same time an endothermic change at the melting point of zinc appeared. The effect of varying the size of

the copper particles was greater than that shown by varying the size of the zinc. Increasing the compacting pressure increased the intensity of the exothermic change up to a pressure of 10 tons/in^2. Above this value the intensity was substantially constant.

From this and other information, they postulated the transfer of zinc through the vapour phase onto the copper particles to form, as has been said, the intermetallic compound CuZn.

Metallographic Methods.

A number of authors have included metallographic studies in their investigations. Butler and Hoare(12) and Barnes(10) have both shown the development of porosity in copper-nickel specimens during sintering by this technique. Due to the amount of porosity to be found in powder compacts, particularly immediately after a reaction forming an intermetallic compound, metallographic preparation and examination can be most difficult. The identification of these inter-metallic compounds in the early stages is not made easier by the fact that they are to be found as thin films or isolatedspots at points of contact between dissimilar grains. These are extremely difficult to see if the surface requires etching due to the difficulty of avoiding staining at the edges of pores. Cranston(17) was able to show the progress of sintering in copper-zinc compacts by metallographic examination, no etching being required. Since isotropic and anisotropic crystals can be distinguished under polarized light, the use of this method as advocated by Mott and Heines(13) would allow specimens from certain

other systems to be examined in the unetched state.

It would seem, therefore, that by using the correct techniques, metallography can be of use in studying the progress of alloy-sintering, at least during the later stages, when the porosity is not extremely high, and the phases present are fairly well developed.

X-Ray Methods.

X-ray crystallographic techniques have generally been used to explain more fully observations made by one of the previous methods though it should be possible to study the complete process of alloy-sintering by this method.

In their investigation of the sintering of the copper-gold system Dawes and Jordan(14) found that in a compact containing 25 at.% Au the intermediate phase CuAu formed at 315°C. This ordered phase remained in apparent equilibrium with the residual copper, until the order-disorder transformation temperature of CuAu had been exceeded. Above this temperature the normal solid diffusion processes gradually resulted in the formation of a homogenous solid solution of gold and copper.

Rhines and Colton(19) reported the formation of intermediate phases in copper-zinc and copper-tin compacts during sintering. In a copper-zinc compact containing 30% Zn heated to 400°C they identified α brass and the η compound. Similar behaviour was observed during the heating of a copper-tin compact, although the process was more complicated owing to the numerous intermediate phases found in this system.

As has already been mentioned, Howat, Craik and Cranston(16) claimed that in the copper-zinc system, one intermetallic compound was formed, independent of the composition, from 10% to 50% Zn. From X-ray studies they concluded that this compound was the β phase. This compound was observed to form first at 170°C and marked, they said, the initial stage of sintering. This was observed to happen even where the α phase would be expected from a consideration of the equilibrium diagram. In such cases, however, the α phase, did not begin to form until almost all the zinc had been transformed into the β phase.

Studies using Vacuum Deposition Methods.

Since, in the present investigation use has been made of this technique to prepare specimens, it is appropriate to consider the literature dealing with vacuum deposition and the results to be obtained by it.

It has been shown by Michel(20) that in certain systems, alloys are formed when the vapours of the two metals are successively deposited on a cold target (20°C). Silver-tin and silver-zinc are examples of this type. On the other hand other systems, such as silver-magnesium and copper-gold will not give alloys under these conditions.

When Michel(21) vaporised copper and gold simultaneously from two filaments onto a series of collodion targets, arranged so that the composition of the deposited layer would change from copper to gold, he found that a solid solution was formed in which the parameter varied in a continuous manner with the composition. This is as would be

expected of copper-gold alloys from consideration of the equilibrium diagram. Goldsztaub and Michel(22) examined the system silver-magnesium by the same method and found that the various intermediate phases were formed, depending on the positioningof the target.

Michel(23) also investigated the structures of films obtained by depositing copper and aluminium vapours on targets of collodion or rock-salt. When the metals were vaporized successively only the two pure metals were found. However, he claimed that by simultaneously vaporizing the two metals, alloys could be obtained. Takahashi and Trillat(24) made a fairly detailed study of this system using a modification of Michel's method and found that when a cold target was used a mechanical mixture of the two metals was obtained, even when the metals were simultaneously vaporized. By aging at room temperature or at an elevated temperature, or by depositing the vapour onto a heated target intermetallic compounds were formed. From 0 to 50% Cu a solid solution of copper in aluminiumand the phase $CuAl_2$ were observed. In certain cases the $CuAl_2$ was in a modified form. From 60% to 100% Cu they claimed to have observed a phase "η" with the CsCl type of structure which is the basis of the CuAl and Cu_9Al_4 phases but which is not found in the equilibrium diagram. In addition to this phase there appeared traces of $CuAl_2$, CuAl, Cu_9Al_4 and copper, depending on the composition of the film.

Howat, Greik and Cranston(16) have shown that in the copper-zinc system one intermetallic compound forms over a wide range of composition at a low temperature. This is believed to be associated with the transfer of zinc onto the copper particles through the vapour phase. In view of these results it was decided to investigate other binary systems containing intermediate phases to discover if this were a general phenomenon. Particularly, it was desired to know if intermetallic compound formation of this type would occur in systems where the vapour pressures of both metals were low enough in the temperature range under consideration to rule out the possibility of one being transferred through the vapour phase.

Differential thermal analysis was chosen to examine compacts for the possible occurrence of intermetallic compound formation, as it seemed to be less influenced by extraneous factors such as the escape of entrapped gases and expansions caused by unequal rates of interdiffusion, than was dilatometric examination.

An investigation of the crystallographic structure of compacts after various sintering treatments would also be made to confirm the results obtained by differential thermal analysis.

The details of these techniques will be described in the following Chapter.

CHAPTER III.

EXPERIMENTAL TECHNIQUES.

EXPERIMENTAL TECHNIQUES.

Preparation of Compacts.

The compacts used throughout the experimental work were prepared from mixtures of metallic powders having the screen characteristics shown in Table I. (B.S.S. screens have been used throughout this investigation).

TABLE I.

Details of Powders.

Metal	Powder	Supplier	Size
Nickel	Carbonyl	Powder Metallurgy	-300
Magnesium	Atomised	B.D.H.	-150 (95% -200)
Tin	Atomised	Powder Metallurgy	-300
Zinc	Atomised	Powder Metallurgy	-200
Aluminium	Medium Size Grease free	B.D.H.	90% -200
Copper	Oxide powder hydrogen reduced.	B.D.H.	-150 #
Iron	Electrolytic	George Cohen	-150 #

* Erroneous results were at first obtained with the copper-aluminium and iron-aluminium systems, due to the presence of oxide films on the copper and iron powders leading to an alumino-thermic reaction. As a result all copper and iron powders were given a reducing anneal in hydrogen before use. For copper the temperature was 450°C, and for iron 600°C, the time of reduction for both metals being 4-8 hours, followed by cooling in hydrogen. The powders were then kept in a dry atmosphere until required for use.

As a result of this treatment partial sintering of the powders took place. Light grinding with a pestle and mortar served to break down the aggregates so formed. Of the -150 mesh powder, approximately 90% was -200 mesh. Since the powders were originally -300 mesh it is possible that particles larger than this size were composed of a number of small particles joined to one another by necks. The surface area of these particles would thus be greater than usual.

Weighed quantities of the required metal powders were carefully mixed and transferred to a steel mould, 3 5/8 ins. external dia., 1.150 ins. internal dia. and 4½ ins. long having a tapered base plug 1 3/8 ins. deep. In this the mixed powders were compressed under a given load, the load being maintained for at least 3 mins. to ensure a standard compaction. In the differential thermal analysis experiments the compacting pressure was 50 tons/in^2. the nominal weight of the

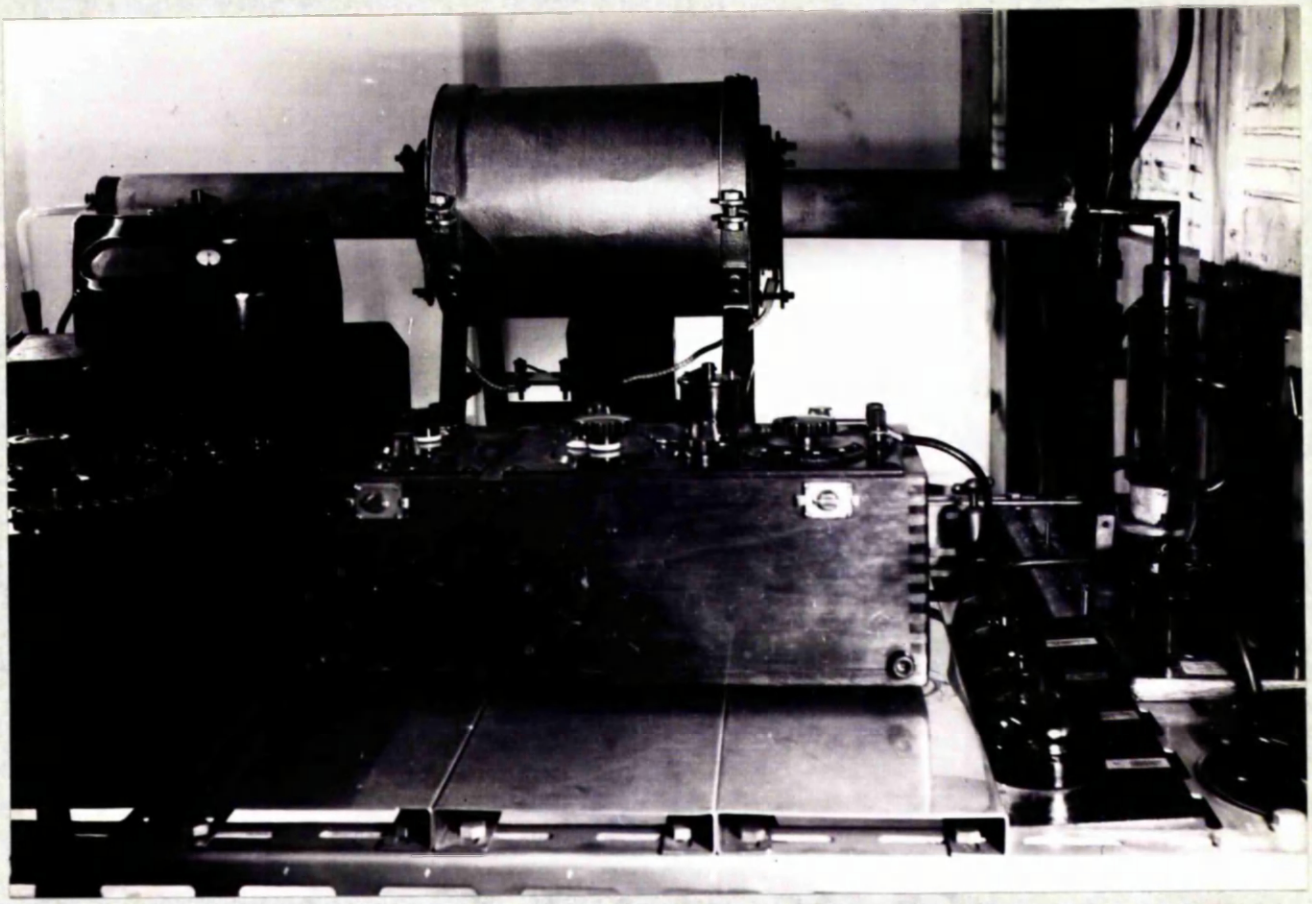

FIG. 1A; GENERAL VIEW OF THE APPARATUS FOR DIFFERENTIAL THERMAL ANALYSIS.

compact normally being 20 gms. although 30 gm. compacts were necessary in those systems containing two heavy metals. After compaction a small hole was drilled radially along the diameter from the edge to the centre of the compact.

The 10 gm. specimens for annealing prior to X-ray analysis were also pressed at 50 tons/in.^{2} Before use they were generally quartered so giving four similar specimens from each compact.

Specimens to be used for the vacuum deposition experiments were 1·5 gms. in weight and were compacted at only 5 tons/in^2. to yield as open and porous a compact as possible. It was argued that entrapped gases could more easily be removed from such specimens and that the metal vapour would penetrate more deeply. The small thickness allowed quick heat transfer and enabled strips from the compact to be used for X-ray powder photographs.

It should be noted that in the course of the present investigation, weight percentages have normally been used in referring to the composition of specimens. Thus, unless otherwise stated, all compositions in this thesis are given in weight percentages.

Differential Thermal Analysis.

The differential analysis curves were obtained by comparing the rate of heating of the test specimen and a standard of similar size and shape in a Nichrome wound furnace as is shown in Fig.1a.

The mullite furnace tube was sealed at both ends by tight fitting rubber bungs, one of which was pierced by a short wide bore copper tube leading to a Metrovac type 02B oil diffusion pump, backed by a

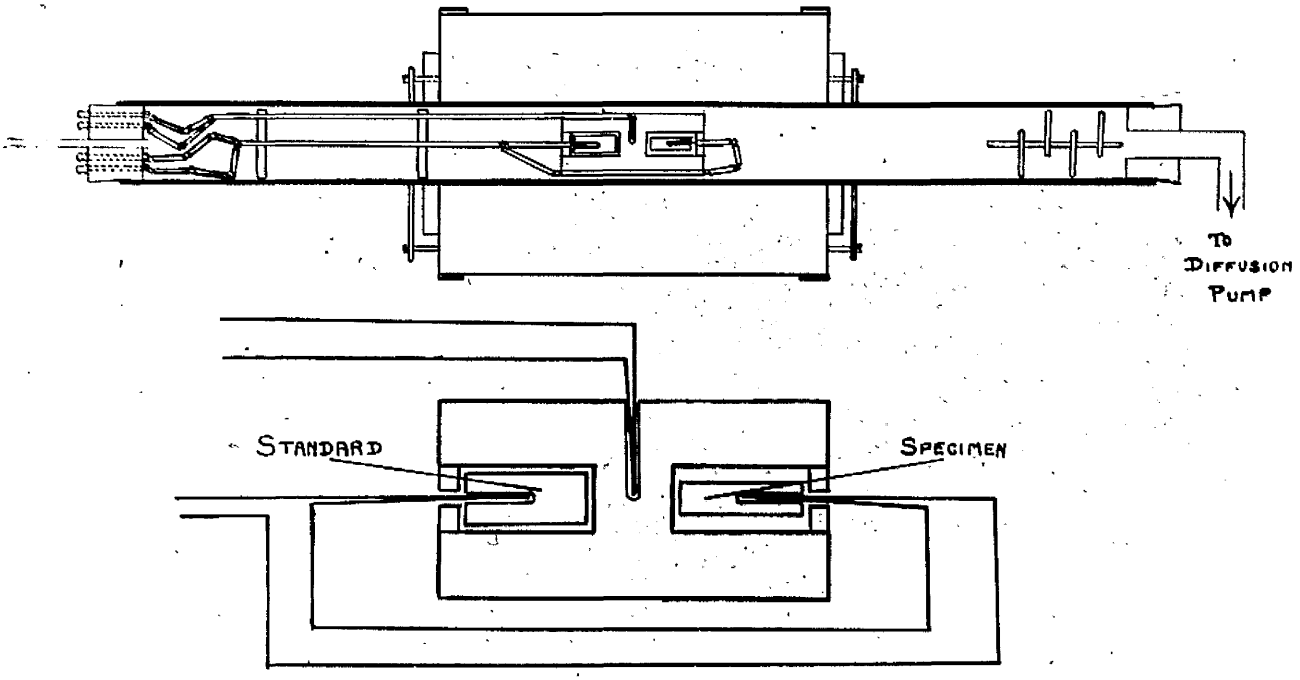

FIG. 1B; THE ARRANGEMENT OF THE THERMOCOUPLES IN THE APPARATUS FOR DIFFERENTIAL THERMAL ANALYSIS.

Metrovac type S.R.2 rotary pump. Baffles just inside the furnace tube prevented any condensed metal vapours, loose powder, etc., being carried over into the diffusion pump. At the other end the thermocouple leads were carried through the bung by brass rods. This bung was also pierced by a glass tube which was coupled to a Pirani gauge or to a McLeod gauge. Before use all joints were sealed with a solution of Pyroxelin in amyl acetate. In this way a pressure of the order of 5×10^{-4} mm. Hg. could normally be obtained up to and beyond the temperature of the heat evolution.

The alundum container, Fig.1b, had a slot cut in each end to carry the standard and test specimens, a small cover of alundum being provided for each slot. The temperature of the container was measured at a point midway between the two slots by a chromel-alumel thermocouple. The standard was a disc machined from copper, copper being used on account of its relatively high melting point, its freedom from phase changes and its slow rate of change of specific heat with temperature. It was equivalent in size to the largest test specimens used and so was considerably heavier than them, weighing just over 50 gms. Even though the standard was sited as far from the test specimen as possible, there was a tendency for its temperature to rise slightly during a large exothermic heat evolution in the test specimen. This tendency is further reduced by increasing the weight of the standard specimen. Like the test specimens it had a hole drilled along a diameter from the edge to the centre to take one junction of the alumel-chromel-alumel differential thermocouple.

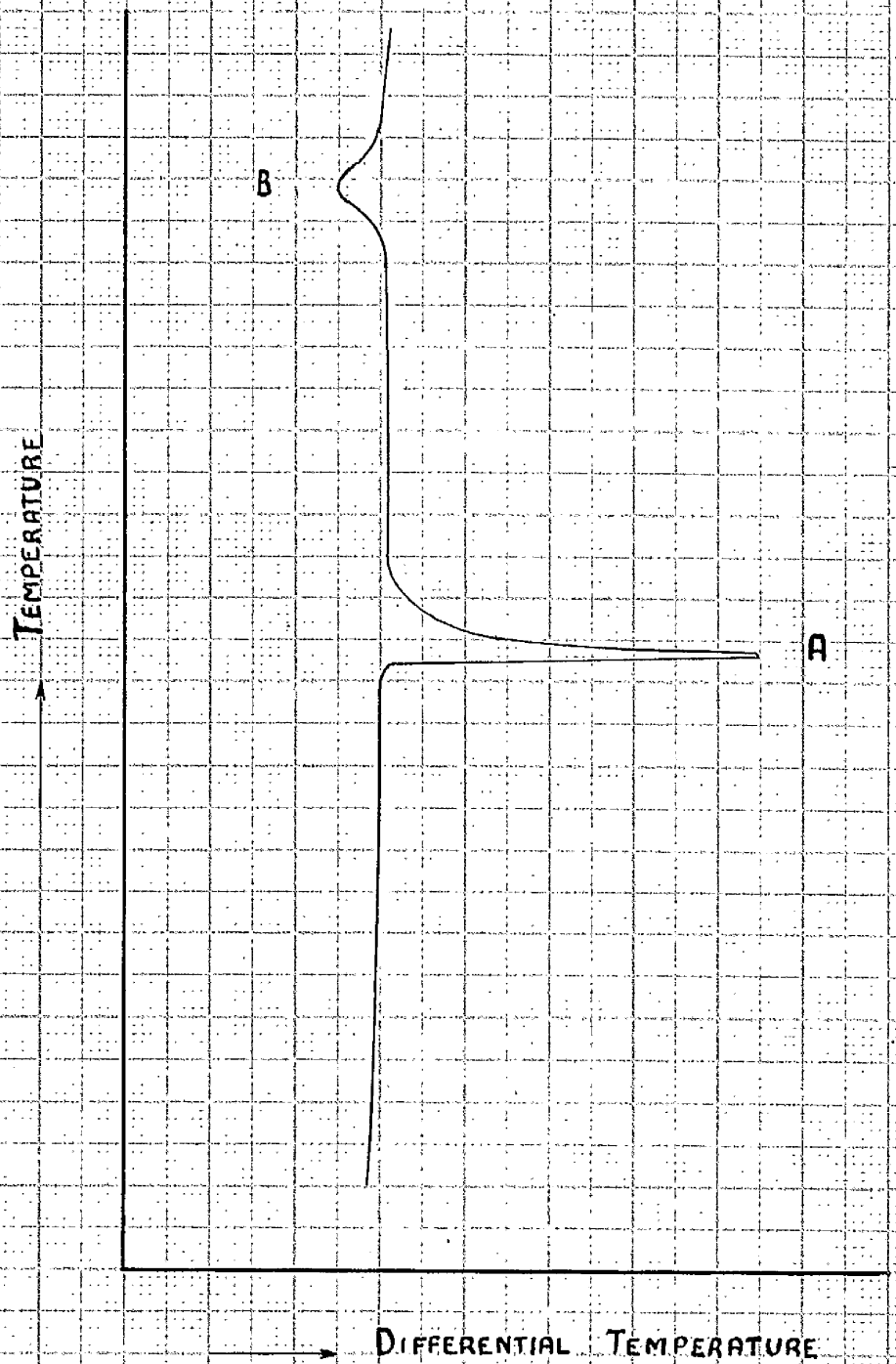

FIG. 2.

GENERAL FORM OF CURVE OBTAINED BY DIFFERENTIAL THERMAL ANALYSIS.

The differential thermocouple leads were taken to a Tinsley vernier potentiometer, coupled with a Cambridge spot galvanometer, reading to 0.01 mV. The furnace temperature was measured on a Cambridge portable potentiometer.

Readings on the differential thermocouple were taken every 0.1 mV temperature rise, while the furnace was controlled to a heating rate of 20°/Min. by a Variac transformer. The heating rate was allowed to slow up to 10°/Min. for the last 150C° before an expected heat change.

The readings obtained from the differential thermocouple were plotted against the temperature of the container. With a constant heating rate the differential thermocouple should read zero or some other steady value but in practice a small amount of drift is sometimes obtained. However, if a reaction occurs in the test specimen, either endo- or exothermic, the differential couple will show the temperature difference between the standard and test specimens. The standard specimen should be unaffected by the heat change if a true reading is to be obtained. This is provided for in the positioning of the specimens in the alundum container and by the relatively large mass of the copper standard.

The general form of the graph which is obtained is shown in Fig.2, which illustrates the straight initial portion and an exothermic reaction at A caused by the metal powders reacting to form an intermetallic compound. As a rule it is found that this reaction occurs over a very small temperature range, indicating that the alundum container and the copper standard are little affected by the heat evolution in the test

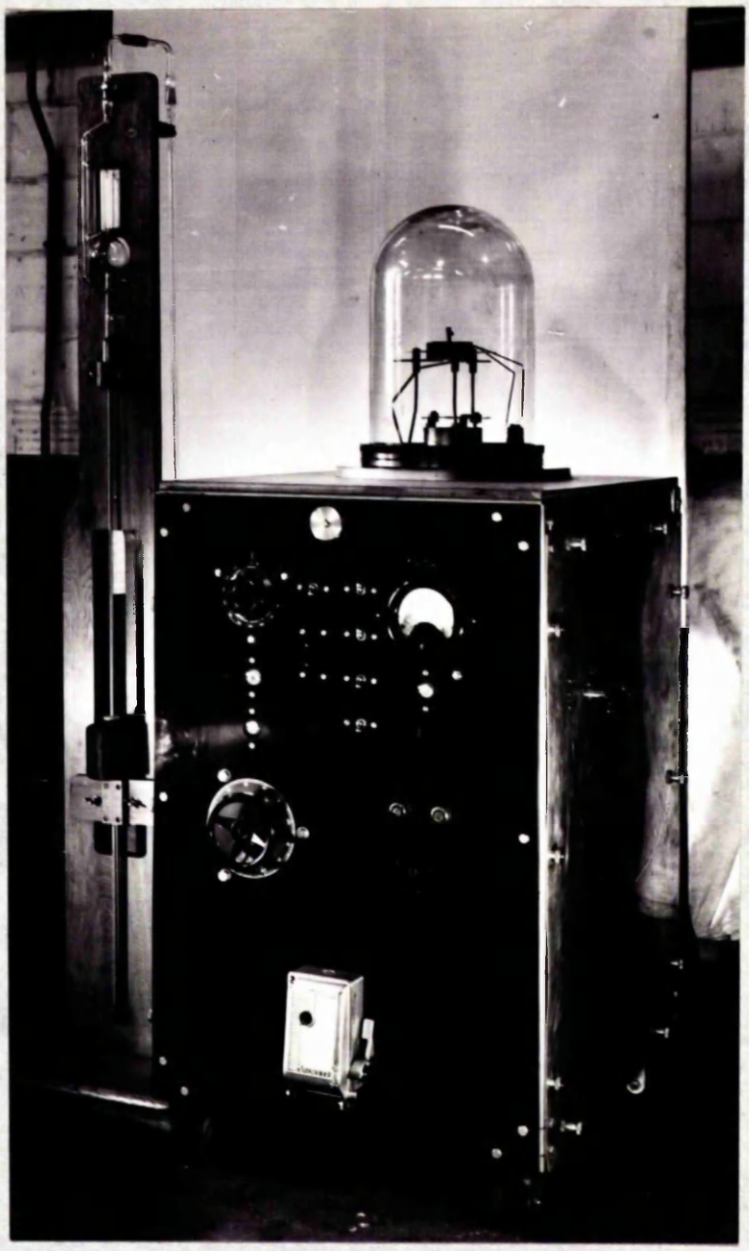

FIG. 3; GENERAL VIEW OF THE APPARATUS FOR VACUUM DEPOSITION.

specimen. For this reason it is believed that the maximum differential thermocouple reading can be taken as a reliable measure of the magnitude of the heat change. At a higher temperature, at B, there can be seen a small endothermic change such as that caused by the melting of a metal which has been present in excess.

Vacuum Deposition.

In this method a metal is heated in vacuum until it evaporates and the vapour condensed in the form of a thin film on a specially prepared target. A general view of the apparatus which was used can be seen in Fig.3. The pumping system comprised a Metrovac type 03B oil diffusion pump and a Metrovac type DR1 rotary pump. A baffle valve was interposed between the bell jar and the diffusion pump to allow the vacuum in the bell jar to be broken without the necessity of shutting off the diffusion pump. Test specimens could be removed from and introduced to the bell jar as often as necessary because of the arrangement of a by-pass line and valve enabling the bell to be evacuated directly by the rotary pump. The baffle valve connecting the diffusion pump was opened only when the vacuum in the bell had reached a low value.

The controls for the valves between the rotary pump and the diffusion pump and on the by-pass line to the bell jar are seen on the right side of the unit, the controlfor the baffle valve being at the top centre of the front panel in Fig.3.

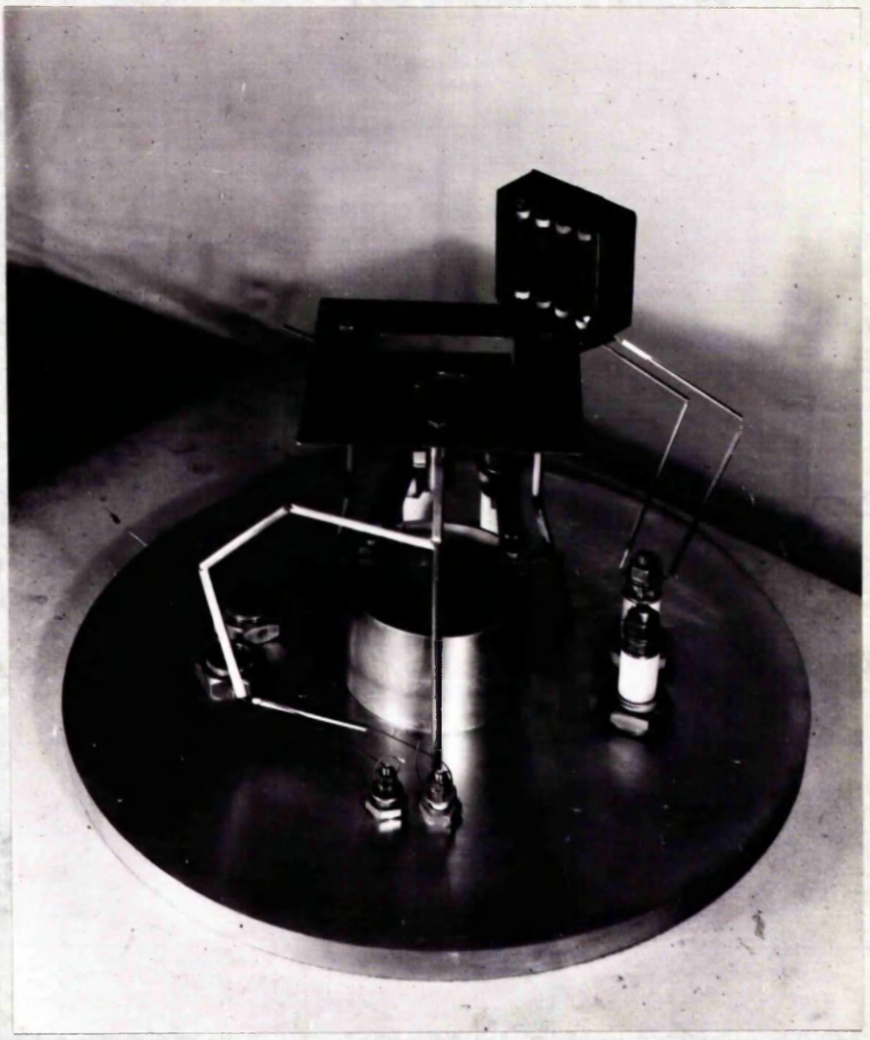

FIG. 4; DETAILED VIEW OF THE APPARATUS FOR VACUUM DEPOSITION.

The pressure in the bell was measured by a Pirani gauge which was calibrated and checked by a McLeod gauge. The pressure reached before evaporationwas commenced was generally 10^{-5} mm. Hg. and was always less than 10^{-4} mm.

The metal to be evaporated was placed on a tungsten filament held between copper bus-bars above the centre of the base plate as can be seen in Fig.4, which gives a detailed view after the bell-jar has been removed. It was found that the most suitable type of filament was one composed of a number of strands of $\frac{1}{2}$ mm. wire, bound together by very fine wire.

A short wide metal cylinder was arranged just under the filament to protect the insulated terminals from metal vapour. In addition, it was found necessary to place a glass cylinder (not shown in the Figure) round each of the terminals supplying current to the target heater, as shorting resulted from the formation of the slightest metal film on the insulator. This risk was considerably smaller with the terminals supplying current to the filament since they had only 12 volts applied to them. The winding of the target heater was also protected from the metal vapour by a guard.

The target, a compact whose preparation has already been described, was supported by three arms at a point $3\frac{1}{2}$ ins. above the filament One of these arms was a chromel-alumel thermocouple enclosed in a sheath. Since the target rested on the actual junction of the thermocouple, a reliable measure of the temperature of the undersurface of the target was

obtained. The target could be raised to any temperature in the range 0-500°C by heat radiated from the spiral windings of a small flat furnace arranged just above the target and supported on the same arms. The current passing through the windings is controlled by a variac transformer. In Fig.4, this heater is shown sitting on its side on the framework of the target support. The guard for the undersurface of the heater can also be seen surrounding the specimen.

When the heater was not in use there was little rise in temperature of the specimen during deposition of the metal vapour. In 20 sec. the normal time of deposition, the temperature as recorded by the thermocouple under the specimen and thus subject to radiation from the filament rose by about 20 °C. However, a thermocouple placed above the specimen showed no increase in this time. A similar rise was found even when the target was heated to a given temperature by the small flat furnace.

In the experiments with copper and aluminium the copper target was a 1.5 gm. compact, 0.3 mm. thick, and a layer of aluminium 0.01 mm. thick was deposited after 20 secs. vaporisation.

X-Ray Crystallographic Analysis.

(a) Partially sintered compacts.

The compacts, covering a range of compositions in any one system, were heated for the same length of time at a series of constant temperatures. Similar tests were made with different sintering times. Normally fresh ppecimens were used for every experiment, though occasionally specimens sintered at one temperature were subsequently sintered at higher temperatures.

The sintering was carried out in a two inch mullite tube in a Nichrome wound furnace. The furnace was controlled by a Kelvin-Hughes controller in conjunction with a Variac transformer, giving an accuracy of ± 20°. The tube was continuously evacuated by an Edwards Hyvac pump to a pressure of 10^{-3} mm. Hg.

After sintering the vacuum was released and the specimens quickly quenched in water. The surface layers were removed from the specimens with a very fine file, after which the filings were collected and passed through a 200 B.S.S. sieve. The X-ray specimens were made by packing this powder into a Vitreosil tube of approximately 0.3 mm. bore. The specimen was then mounted in a 9 cm. Unican powder camera and fitted to a Newton Victor Raymax unit of the rotating anode type. Generally copper radiation, filtered through nickel was used, but for systems containing iron, cobalt radiation was used, with an iron filter.

Metals and intermediate phases were generally identified by comparing the observed lines with the lists of interplanar spacings contained in the A.S.T.M. Card Index. Since true Angstrom units have been used throughout this investigation to express interplanar spacings and parameters, it was necessary to multiply the values in the Card Index by a factor of 1.00202 to correct the wavelength in the Siegbahn Tables.

The intensities of the lines in these cards are given as a fraction of the intensity of the strongest line (I/I_1), this intensity (I_1) being taken as unity. The intensities of the lines observed in this investigation are visually estimated. Since the angle at which any line

appears is different with copper or cobalt radiation from that at which it would appear with the molybdenum radiation used for many substances in the Card Index, the polarising factor will be different, so altering the intensity of the line. Differences in the source of the specimen and in its preparation can also alter the relative intensities of the lines.

In many cases samples of intermetallic compounds were prepared by fusion in a high frequency induction furnace, in order to give standards against which films from partially sintered compacts could be compared. In addition, the parameters of most of the intermetallic compounds found were evaluated, using Nelson and Riley's function(25) to extrapolate the value of a_o.

(b) Specimens from vacuum deposition experiments.

When the target had been removed from the bell-jar a narrow strip of cross-section 0.3 x 0.6 mm. was cut from it, and mounted in the same 9 cm. Unicam camera as before. On account of the fairly large cross-sectional area of the base metal, the lines generated by it were very broad in the resulting film. The amount of background scatter was also considerably above the normal. However, lines resulting from the evaporated film were fine, due possibly to the small cross-sectional area of this film. In certain cases prior to X-ray examination the whole target or a part of it was subjected to a period of annealing in the furnace described in the preceding section.

CHAPTER IV.

EXPERIMENTAL RESULTS.

EXPERIMENTAL RESULTS.

COPPER-ZINC.

The work of Howat, Craik and Cranston(16) has already been referred to in an earlier Chapter. As a result of their comprehensive investigation into the sintering of compressed copper and zinc powders they concluded that the first compound to form is Cu Zn, the β phase. This compound has a body centred cubic crystal structure, conforming to the Electron Concentration Rule formulated by Hume-Rothery.

In the course of the present investigation, experiments were made on the sintering of copper-zinc compacts using the differential thermal analysis technique.

TABLE II.

Differential thermal analysis of copper-zinc compacts.

Composition Cu	Zn	Corresponding Compound.	Compacting Pressure t/in².	Reaction Temperature °C.	Magnitude of exothermic change °C.
54	46	Cu Zn	10	237	19
54	46	Cu Zn	25	240	34
54	46	Cu Zn	50	212	45
39	61	Cu_5Zn_8	50	200	38

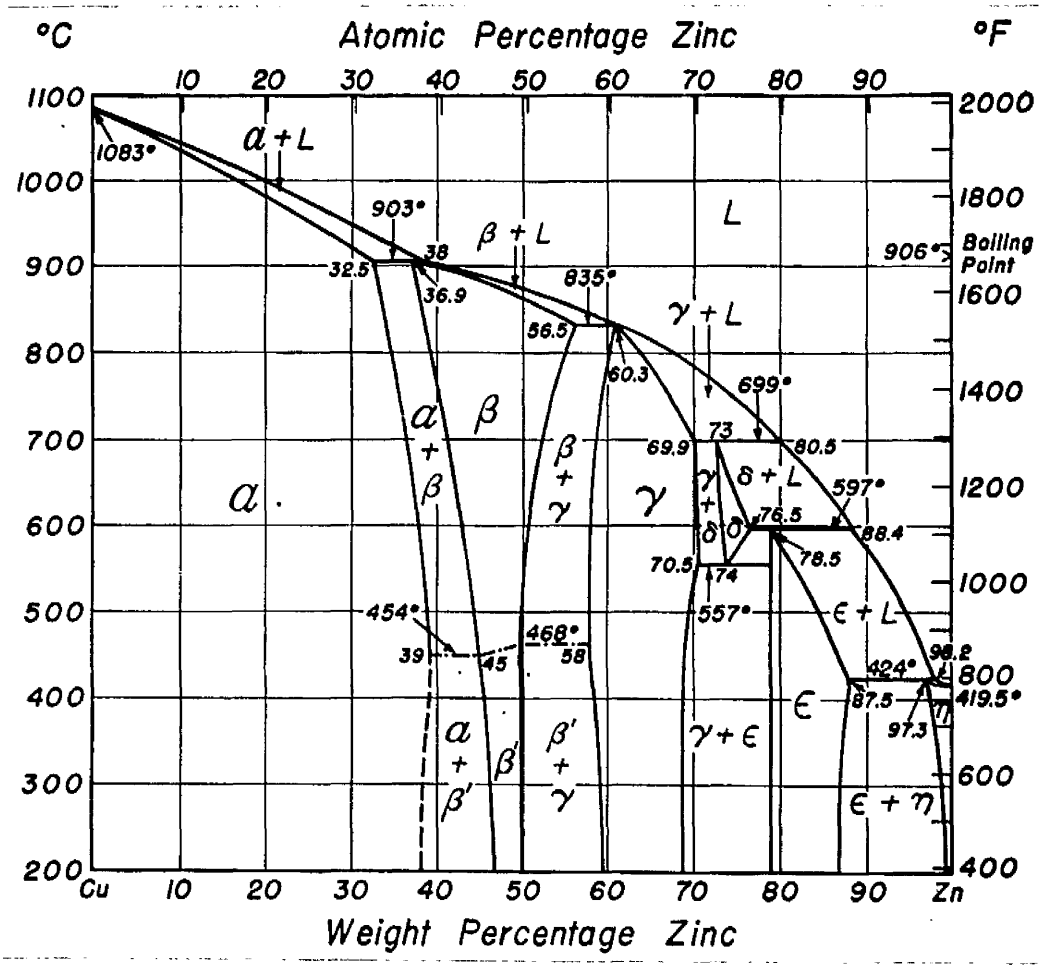

FIG. 5; COPPER - ZINC EQUILIBRIUM DIAGRAM[26].

The results obtained are given in Table II. As will be seen they confirm Howat, Craik and Cranston's findings concerning the effect of compacting pressure on the observed heat change. They also show that the magnitude of the change falls when the composition of the compact is altered from 46% to 61% Zn, i.e., from the composition corresponding to CuZn to that corresponding to Cu_5Zn_8 (Fig.5). This is in accordance with the conclusion that CuZn is the first compound to form.

In view of these interesting results it was decided to investigate the system Nickel-Zinc which contains similar electron compounds to copper-zinc.

NICKEL-ZINC.

In this system, while the β phase similarly forms by a peritectic reaction, the γ phase, Ni_5Zn_{21} has a congruent melting point, unlike its analogue in the system copper-zinc as can be seen in Fig.6(27). At high temperatures the structures of the corresponding compounds are similar, though the β phase transforms to a tetragonal structure at temperatures below 800°C. and a solid state transformation has been reported over part of the composition range of the γ phase.

A series of differential thermal analysis experiments gave the results shown in Table III. The temperature at which the reaction occurs is higher than that in the previous system, being in the neighbourhood of 900°C. The maximum heat evolution occurs in the compact containing 77% Zn, corresponding to the compound Ni_5Zn_{21}.

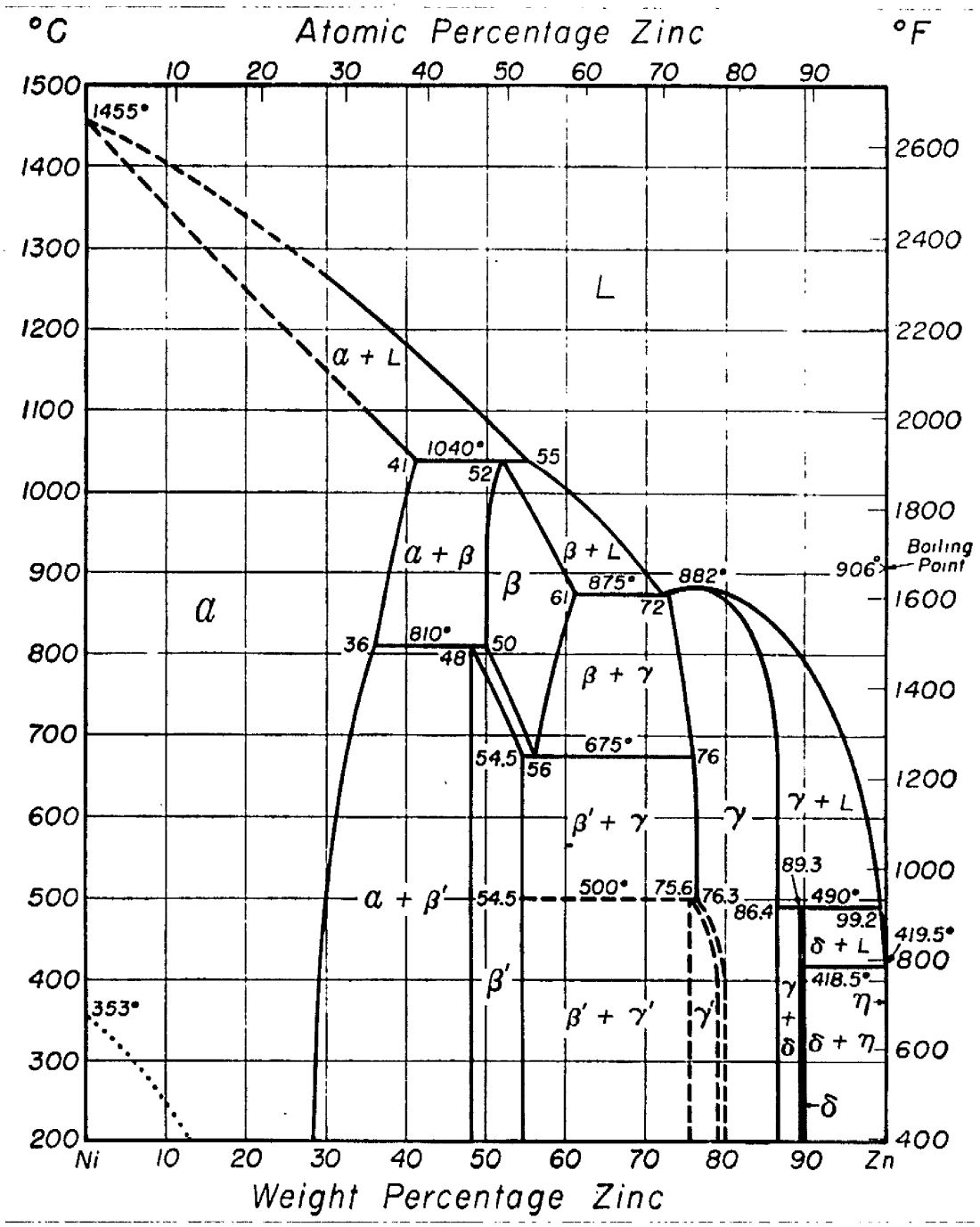

FIG. 6; NICKEL - ZINC EQUILIBRIUM DIAGRAM.

TABLE III.

Differential Thermal Analysis of Nickel-Zinc Compacts.

Composition Ni	Zn	Corresponding Compound	Reaction Temperature °C	Magnitude of Exothermic Change °C.
74	26	α	295	36
46	54	NiZn	288	206
23	77	Ni_5Zn_{21}	305	346
10	90	δ	306	63

This result is not analogous to that obtained with the copper-zinc system where the β compound was formed. Ni_5Zn_{21} is, however, given as another compound obeying the Electron Concentration Rule, its structure being that of γ brass.

Since it seemed possible that there might be some factor connected with the congruent melting point in Ni_5Zn_{21} which induced this phase to form first, it was decided to investigate a system containing a compound with a congruent melting point which is stable to a high temperature.

COPPER-ALUMINIUM.

This system was chosen as the β and γ phases have high melting points and occur at the values of e/a indicated by the Electron Concentration Rule. The structures of these two compounds are, as one might

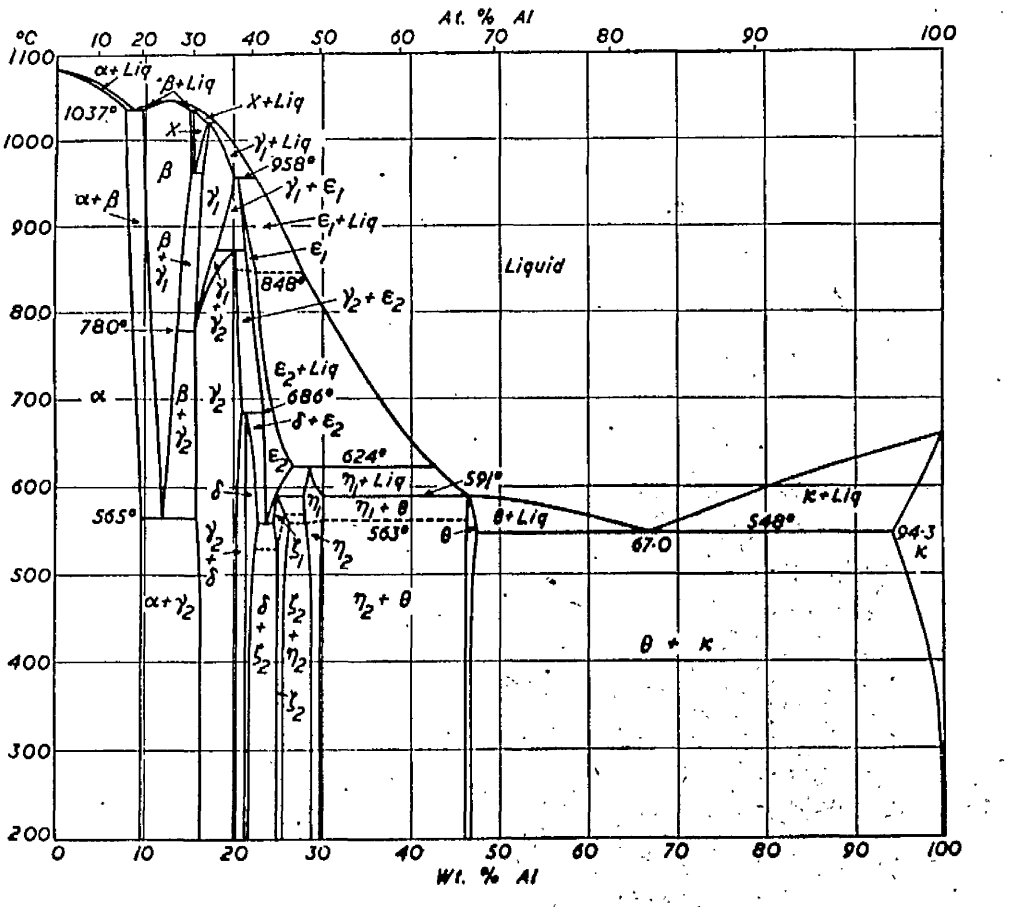

FIG. 7; COPPER - ALUMINIUM EQUILIBRIUM DIAGRAM.

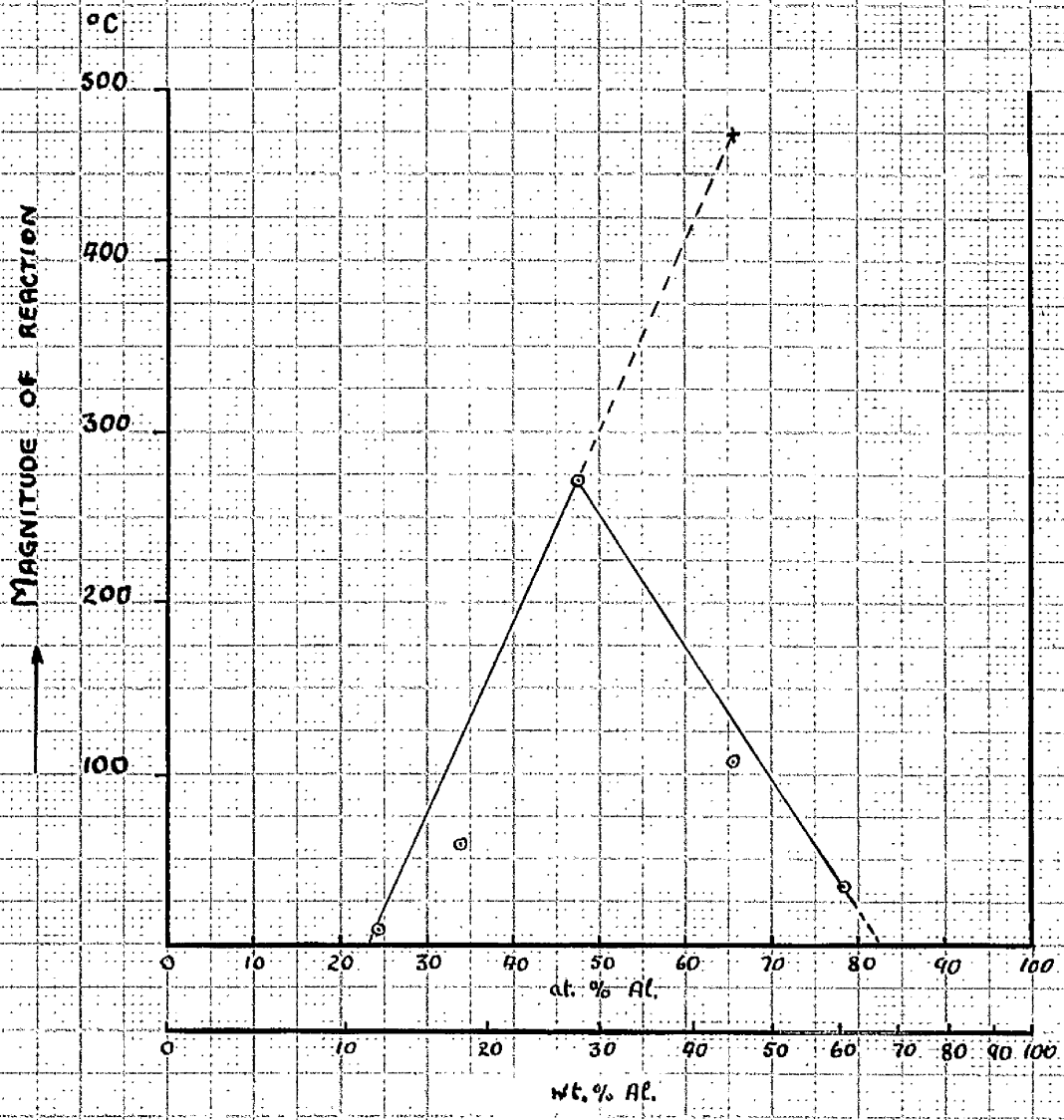

FIG. 8; VARIATION OF THE MAGNITUDE OF THE EXOTHERMIC REACTION WITH THE COMPOSITION OF THE COMPACT IN THE COPPER – ALUMINIUM SYSTEM.

expect, similar to those of the analogous compounds in the previous two systems. As can be seen from Fig.7(28), the β phase Cu_9Al has a congruent melting point and in fact has the highest melting point of all the intermetallic compounds in the system. It might therefore be thought, from the results of the previous two systems that Cu_9Al should be formed first during the sintering of copper and aluminium.

Differential Thermal Analysis.

However, as can be seen from Table IV the maximum heat change observed in differential thermal analysis occurs in a specimen containing 28% Al, corresponding to $CuAl(\eta)$. This phase has an orthorhombic structure and forms in a peritectic reaction at a comparatively low temperature. These results are illustrated in Fig.8, which shows the change in magnitude of the exothermic reaction with change in composition of the compact. The dotted extrapolation of the line joining the copper rich specimens to temperatures greater than 272°C is not due to experimental results and reference will be made to this at a later stage.

TABLE IV.

Differential Thermal Analysis of Copper-Aluminium Compacts.

Composition Cu	Al	Corresponding Compound	Reaction Temperature °C	Magnitude of Exothermic Change C°
88	12	Cu_9Al	490	7
82	18	Cu_9Al_4	470	57
72	28	$CuAl$	460	272
55	45	$CuAl_2$	448	112
40	60	-	525	35

The specimen containing 28% Al, which gave the maximum heat change was examined by X-rays after the completion of the experiment. It was found to contain copper, aluminium, $CuAl_2$ and Cu_9Al_4. No lines were observed which could be identified as orthorhombic CuAl.

Takahashi and Trillat(24) have reported the formation of an ordered body centred cubic structure of composition CuAl in evaporated films of copper and aluminium. None of the lines observed in the photograph of the 28% Al specimen could be identified with this structure.

The presence of $CuAl_2$ and Cu_9Al_4 in a specimen whose composition corresponds to CuAl is somewhat surprising. It might now be thought that Cu_9Al_4, the γ phase, was the first compound to form. It can be seen, however, from Table IV that the observed heat change in the 18% Al specimen, corresponding to Cu_9Al_4 is considerably less than that observed in the 45% Al specimen, corresponding to $CuAl_2$.

If the temperature rise recorded by the differential thermocouple be added to the temperature at which the reaction begins then as a result of the heat generated by the exothermic reaction compacts containing 45% and 60% Al may reach a temperature of 560°C, i.e., just above the eutectic formed between $CuAl_2$ and Al. There is, therefore, the possibility that some quantity of liquid phase may form in these compacts as a result of the heat generated by the reaction. The formation of this liquid phase with the absorption of latent heat of fusion may profoundly influence the magnitude of the heat change as recorded by the differential thermocouple.

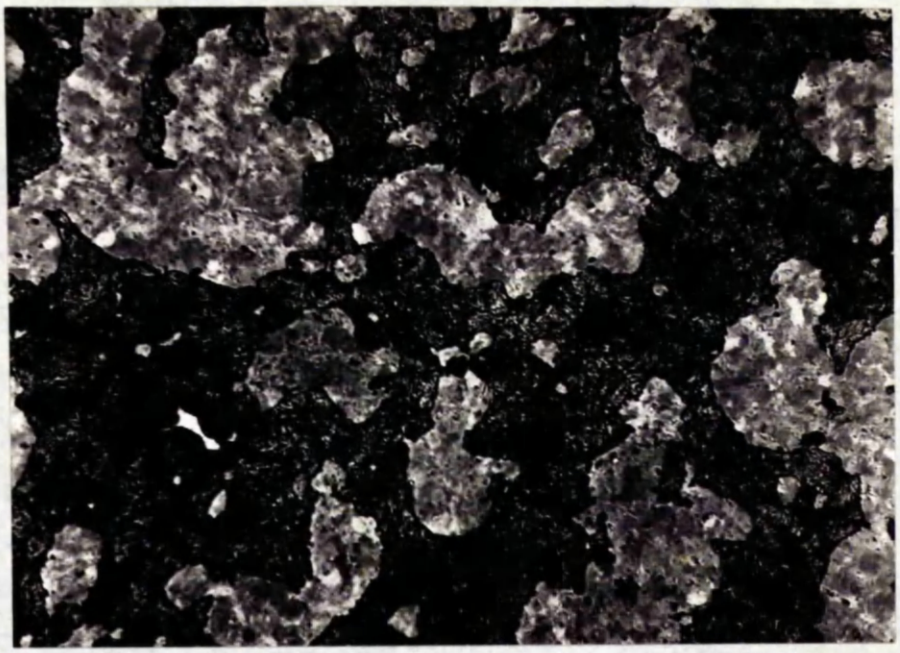

FIG. 9; a) A COPPER - ALUMINIUM SPECIMEN CONTAINING 70% AL. ETCHED WITH AN ACID SOLUTION OF FERRIC CHLORIDE. X 110

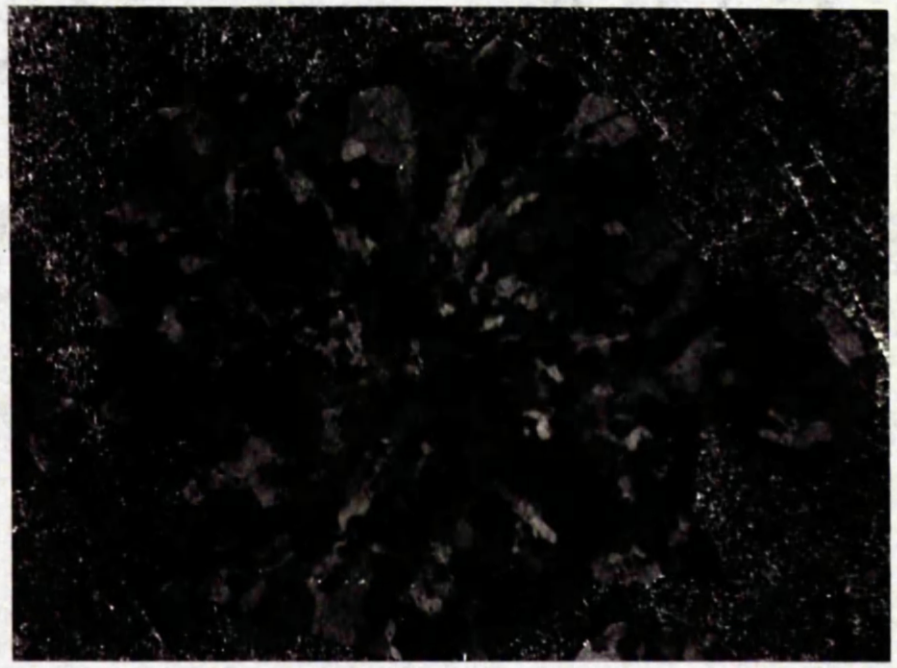

FIG. 9; b) THE SAME SPECIMEN IN THE UNETCED CONDITION. EXAMINED UNDER POLARISED LIGHT. X 400

Thus the magnitude of the exothermic reaction should be greater than that actually observed, and certainly considerably greater than that observed in the 18% Al specimen.

To investigate this possibility further it was decided to examine metallographically specimens containing 40% and 70% Al annealed at 520°C for 75 hours. From Fig.9a, which shows the specimen containing 70% Al, it can be seen that there is very little porosity present, the structure being composed of light grains set in a dark background, having the appearance of a eutectic. Examination at a higher magnification with polarised light (Fig.9b) shows that the grains are anistropic while the background is isotropic. According to X-ray analysis this specimen contains only $CuAl_2$ and aluminium. Since the lattice of $CuAl_2$ is tetragonal and that of aluminium, cubic, it would appear that the structure is grains of $CuAl_2$ set in a background of aluminium.

Judging by the small amount of porosity present, the absence of angular pores and the rounded appearance of the grains of $CuAl_2$ it would seem probable that considerable quantities of a liquid phase have formed during annealing.

The metallographic structure of the specimen containing 40% Al is shown in Fig.10a. It appears to be composed of grains of a light phase set in a background which is similar to the grains of $CuAl_2$ in the last specimen. It will be seen that there is more porosity in this specimen than in the last, but that almost all of it is in, and near, the edge of the light grains. Examination with polarised light at a higher

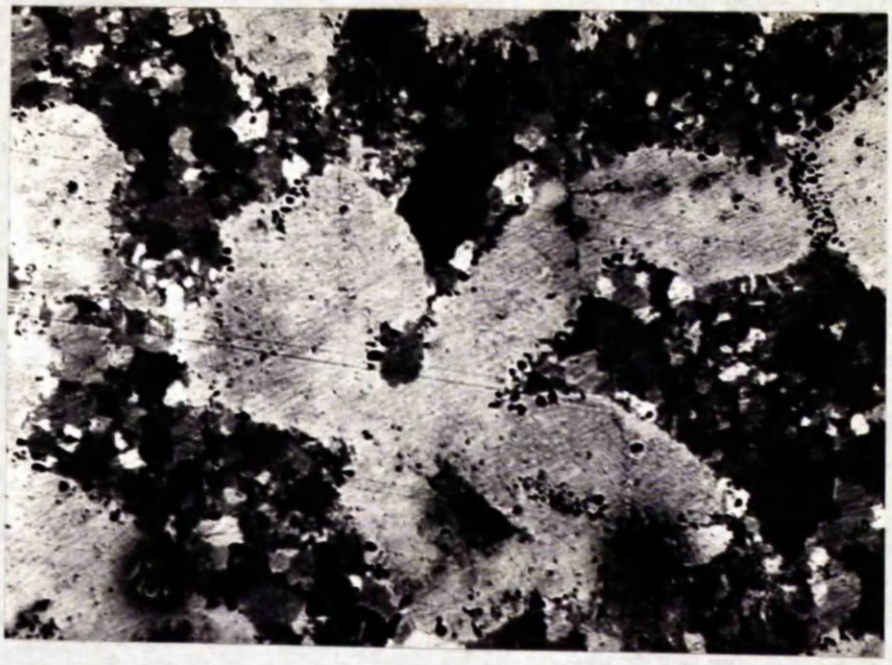

FIG. 10; a) A COPPER - ALUMINIUM SPECIMEN CONTAINING 40% AL. ETCHED IN AN ACID SOLUTION OF FERRIC CHLORIDE. X 140

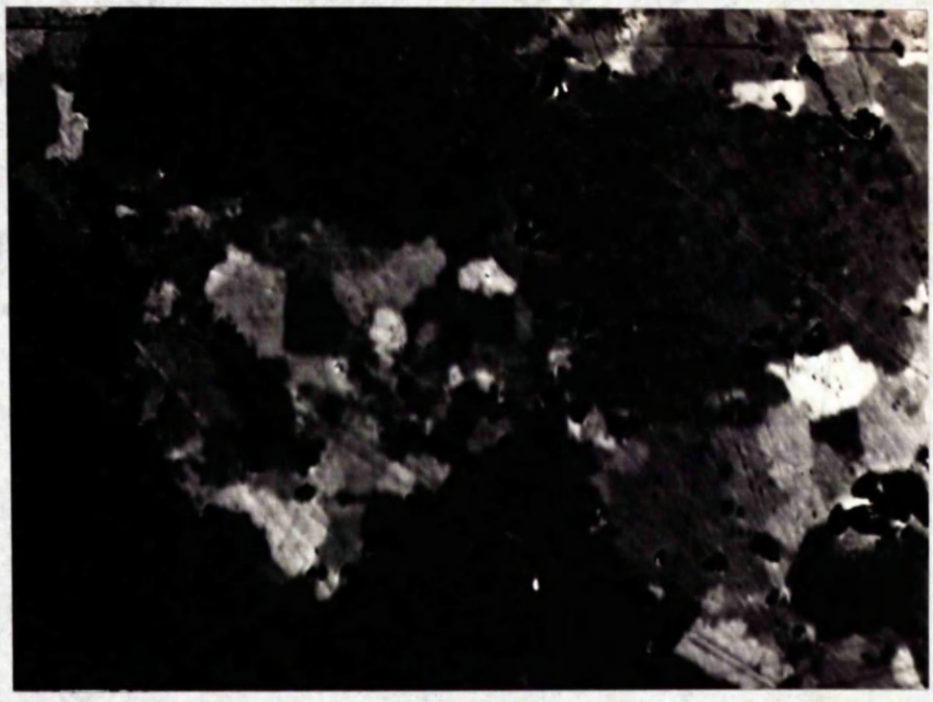

FIG. 10; b) THE SAME SPECIMEN IN THE UNETCHED CONDITION. EXAMINED UNDER POLARISED LIGHT. X 400

magnification (Fig.10b) shows that the grains are isotropic, while the background is anisotropic. The structure of this specimen as revealed by X-ray analysis is Cu_9Al_4, $CuAl_2$ and aluminium. This would be accounted for if the large isotropic grains were Cu_9Al_4, and the background $CuAl_2$. The aluminium would be in the form of small isotropic grains, probably without internal porosity.

Since Cu_9Al_4 has a much higher melting point than $CuAl_2$ and aluminium, it would be less affected by the formation of a liquid phase. In this way porosity would still be found in grains of this compound, whereas porosity would tend to disappear from the $CuAl_2$ and aluminium grains. Thus it would seem quite possible that a liquid phase has also formed in this specimen during annealing.

Returning to the results obtained by differential thermal analysis, it is now possible to explain the structure observed in the 28% Al specimen on the basis that $CuAl_2$ is the compound which forms first.

When the reaction starts, $CuAl_2$ is formed and the temperature rises to 548°C when a liquid phase is formed. This liquid will react with some of the excess copper present and form Cu_9Al_4.

As has been said, the possible formation of a liquid phase in all but the copper rich specimens is bound to influence the magnitude of the exothermic change as recorded by the differential thermocouple. This fact and the X-ray structure of the 28% Al specimen cast doubts on the validity of the conclusion that CuAl is the first compound to form.

TABLE V.

Structures observed during the sintering of several copper-aluminium alloys.

10% Al.

Temp. °C.	Time hours.	Copper	Cu_3Al	Cu_9Al_4	$CuAl_2$	Aluminium
400	65	Strong	-	Faint	Weak	Faint
400	103	Strong	-	V.Weak	Weak	Trace
500	74	Medium	-	Medium	-	-
520	75	Medium S.S.	-	Medium	-	-
560	28	Strong S.S.	-	Medium	-	-
650	46	Weak S.S.	Medium	-	-	-

12% Al (Composition of Cu_3Al)

Temp. °C.	Time hours.	Copper	Cu_3Al β	Cu_9Al_4	$CuAl_2$	Aluminium
480	0.5	Strong	-	-	-	Medium
475	12	Strong	-	Weak	Weak	Faint
515	0.5	Strong	-	-	Faint	Weak
510	12	Strong	-	Weak	-	-
510	24	Strong	-	Medium	-	-
510	72	Strong	-	Strong	-	-
555	0.5	Strong	-	-	V.Weak	Weak
560	28	Medium	S.S. -	Strong	-	-
560	63	Medium	S.S. -	Strong	-	-
610	0.5	Strong	-	Weak	-	V.Weak
650	46	V.Weak	S.S. Medium	-	-	-
665	0.5	Medium	-	Strong	-	-

15% Al

Temp. °C	Time hrs.	Copper	Cu_3Al γ'	Cu_9Al_4	$CuAl_3$	Aluminium
560	28	Weak S.S.	-	Strong	-	-
650	46	-	V.Weak	Strong	-	-

20% Al (Near the composition of Cu_9Al_4)

Temp. °C.	Time hrs.	Copper	Cu_9Al_4	$CuAl_3$	Aluminium.
400	65	Strong	Faint	Weak	V.Weak
400	103	Strong	V.Weak	Weak	V.Weak
425	89	Strong	Weak	V.Weak	V.Weak
500	74	-	Medium	-	-
520	75	-	Strong	-	-
560	28	-	Strong	-	-

40% Al (near the composition of $CuAl_2$)

Temp °C.	Time hrs.	Copper	Cu_9Al_4	$CuAl_2$	Aluminium
400	65	Strong	-	Weak	Medium
400	103	Strong	-	Weak	Medium
500	74	-	Weak	Strong	Weak
520	75	-	Medium	Strong	Weak
560	28	-	Strong	Strong	Weak

70% Al.

Temp. °C.	Time hrs.	Copper	Cu_9Al_4	$CuAl_2$	Aluminium
400	65	Strong	-	Faint	Strong
400	103	Strong	-	Faint	Strong
500	74	-	-	Strong	Strong
520	75	-	-	Strong	Strong
560	28	(melted) - (solid)	- trace	Medium Medium	Strong Strong

X-Ray Crystallographic Analysis.

X-ray data relating to compacts heated at constant temperatures for varying times are shown in Table V. The table shows the relative intensities of the phases present in any one specimen after annealing at a given temperature. The intensities of the phases were estimated by comparing the observed interplanar spacings with those given on the respective cards of the A.S.T.M. Card Index, and with the spacings found in fused alloys. The lowest temperature at which compound formation was observed was 400°C. no compound formation having been observed by annealing at 375°C. It will be seen that $CuAl_2$ appears in all the specimens sintered at 400°C while Cu_9Al_4 appears faintly, only in the copper-rich ones. The presence of appreciable quantities of copper and aluminium shows that the initial reaction has not been completed.

A progressive rise in temperature results in the rapid disappearance of free copper in the compacts with 40 and 70% Al. In the 40% Al specimens Cu_9Al_4 appears as the copper disappears, and, as the temperature is farther raised, increases in intensity. There is also a weakening in the strength of the aluminium lines and an increase in quantity of $CuAl_2$. It is observed that even after a considerable time at 560°C the X-ray structure shows no sign of $CuAl$, being composed of Cu_9Al_4 and $CuAl_2$ in about equal proportions. If allowance be made for the aluminium which is still present, it will be seen that the $CuAl_2$ and Cu_9Al_4 are present in the correct proportions for a two phase field between these compounds.

The case of the 70% Al specimen is similar, though in this case there will be a greater inducement for the copper to form quickly $CuAl_2$

and not remain as Cu_9Al_4. Thus, though no Cu_9Al_4 is detected except in the last specimen, it is presumed that a small quantity, too small to be detected by X-ray spectrography is actually present. This last specimen of 70% referred to here, was sintered at 560°C which is above the temperature of the eutectic between $CuAl_2$ and aluminium. As might be expected the specimen was partially melted. The melted portion showed $CuAl_2$ and aluminium to be present in almost equal quantities, while the solid portion showed in addition a trace of Cu_9Al_4 indicating that the specimen had not yet reached its equilibrium structure.

It will be noticed that the composition seems to jump from $CuAl_2$ to Cu_9Al_4. Takahashi and Trillat(24) give interplanar spacings for a body centred cubic lattice which they call "η" $CuAl_2$ as it does not appear in the equilibrium diagram. However, all the lines of this phase agree with those on the A.S.T.M. Card for Cu_9Al_4, and for the high angles which are omitted from the card, with those observed in a 20% Al specimen, which is wholly Cu_9Al_4. The only difference seems to be that the first two lines (of medium intensity) on the card are missing. Thus it will be seen that it is extremely difficult to distinguish this phase from Cu_9Al_4. Though one or other of the first two lines is missing in some cases where there is only a very small amount of Cu_9Al_4 present, it cannot be said that the "η" phase has ever been identified. Another point which lends support to this is that in the 40% Al specimen, sintered at 560°C Cu_9Al_4 and not CuAl is found along with $CuAl_2$.

In the copper rich specimens, $CuAl_3$ is found at low temperatures and short times of annealing. As the temperature is raised, or the time at the same temperature increased, $CuAl_3$ and aluminium decrease in intensity and finally disappear, while Cu_9Al_4 increases in magnitude. By 500°C the 20% Al specimen contains only Cu_9Al_4. Specimens containing more copper than this continue to show copper lines. With long annealing times at temperatures in excess of 500°C some solid solution of aluminium in copper is observed. Below this temperature the copper lines show a close agreement with those on the A.S.T.M. card for pure copper.

When specimens containing 10%, 11.8% and 15.5% Al were annealed at 560°C, all showed copper solid solution and Cu_9Al_4, in varying proportions. From this it might be concluded that they had been fully sintered and reached their equilibrium structures. However, this structure persisted after annealing at 580°C for a considerable time, when the 11.8% Al specimen at least should have been in the β phase field. On raising the annealing temperature to 650°C the equilibrium structures of these specimens are $\alpha + \beta$, β, and $\beta + \gamma$ respectively. After sintering at this temperature and quenching in alcohol and solid CO_2, the X-ray diffraction photographs shown in Fig.11 were obtained.

Alloys whose compositions range from 10-15% Al undergo a "martensitic" reaction, the martensite being formed by a process, similar to that in steel. Wassermann(29) showed that on rapid cooling of specimens containing 11.9 and 12.4% Al, the disordered β phase transformed above 320°C to an ordered structure which he called β_1. On further cooling this β_1 transformed to β'. However, no information was given about this phase.

(a)

(b)

FIG. 11; X-RAY PHOTOGRAPHS OF TWO COPPER - ALUMINIUM SPECIMENS.

a) 15.5% AL., QUENCHED FROM 650°C.
b) 11.8% AL., QUENCHED FROM 650°C.

The 11.8% Al specimen quenched from 650°C which was wholly in the β region, shows lines which agree very well with those relating to β' given by Bradley and Jones(30), as can be seen from Table VI. They may be correlated with a face centred cubic structure or with a hexagonal structure. In neither case, however, is the correlation sufficiently good positively to identify the structure.

TABLE VI.

Interplanar spacings of 11.8% Al specimen quenched from 650°C.

Line No.	β' Bradley and Jones(25)		Copper α solid solution		Observed spacings.	
	I	d	I	d	I	d
a	S	2.24			W	2.24
b	VS	2.12	VS	2.13	S	2.12
c	VS	2.029			m	2.029
d	VS	1.956			m	1.987
e					f	1.759
f	S	1.300	S	1.295	VW	1.295
g	VW	1.175			f	1.185
h	m	1.111	m	1.104	VW	1.106
i	W	1.061	W	1.057	f	1.061

Bradley and Jones have suggested that the structure of β' is similar to a face centred cube with certain atoms missing. Several other investigators have suggested that the structure is hexagonal. Isaitschew,

Kandinsky and Kurdjumow(31) have given data indicating that the lattice is near to a close packed hexagonal form, which would appear to be quite possible. The results obtained in the present investigation would be in accordance with this structure. Line "e" in Table VI, does not correspond to any of the lines given by Bradley and Jones. It does, however, show a good correlation with either the face centred or hexagonal structure. It would seem possible, therefore, that it is a β line. The reason for its appearance here and non-appearance in the investigation by Bradley and Jones may be found in the differences of specimen source and preparation.

Certain of the observed lines have a greater intensity than those from the data of Bradley and Jones. These lines correspond to a copper solid solution containing about 10% Al. Bradley and Jones have observed that when there is any free copper present most of its lines are superimposed on β' lines. Thus, it seems probable that there is some α copper solid solution present in this specimen in addition to the β' phase.

This conclusion was confirmed by metallographic examination, which showed the presence of some very small grains of copper. It was also observed that the acicular martensitic structure was not well developed. However, the structure obtained by quenching from 650°C persisted even after tempering for 55 hours at 375°C. It was necessary to temper for 27 hours at 550°C before X-ray analysis revealed a change in structure. After this treatment, a find nodular precipitate of the γ phase in α was observed.

On quenching from 650°C the 10% Al specimen behaved very similarly to the 11.8% Al specimen, though as would be expected, more α solid solution was observed in the X-ray structure.

It has been shown by Gawranek, Kaminsky and Kurdjumow(32) that above 12.9% Al, the β_1 phase transforms on cooling to γ', a structure having a different X-ray pattern to that of β'. Its structure is said to be hexagonal close packed, a = 2.606Å, c/a = 1.619 (33). It has also been stated that the β' structure differs from γ' in that the [00.1] direction is at an angle of 2° to the (00.1) plane normal, and the angle between the planes (10.0) and (01.0) differs by about 1° from 120° (31).

The 15.5% Al specimen, was found to contain, on quenching from 650°C Cu_9Al_4 and γ'. The γ' was identified with the aid of a Bunn chart and the value of the c/a ratio for γ' given above.

On the basis of the X-ray data obtained the lattice parameters of Cu_9Al_4 and $CuAl_2$ were determined. Table VII shows the correlation of the interplanar spacings of Cu_9Al_4 in a 20% Al specimen with the corresponding A.S.T.M. Card. This card is, unfortunately, incomplete, ending at a "d" value of 1.184. The "d" values of possible lines at higher angles than this were computed from their N values and the published value for the parameter, 8.702 Å (34). The parameter value derived from the observed figures is 8.697Å.

Table VIII shows the lines observed in the 40% Al specimen and those of the cards for Cu_9Al_4 and $CuAl_2$. The values calculated from these data for the lattice constants of $CuAl_2$, which has a body centred tetragonal structure are, a = 6.051Å, and c = 4.877Å. The published values are a = 6.066Å, c = 4.874Å (34). Since Cu_9Al_4 was also present in this specimen the value of its parameter was also calculated and found to be a = 8.714Å.

TABLE VII.

Interplanar spacings observed in a 20% Al specimen annealed at 560°C.

Line No.	N	Cu_9Al_4 γ brass structure		Observed spacings.	
		I/I_1	d	I	d
a	6	0.7	3.56	W	3.53
b	9	0.7	2.90	VW	2.88
c	18	1.0	2.05	VS	2.05
d	22	0.6	1.857	f	1.858
e	24	0.7	1.779	VW	1.777
f	36	0.8	1.453	W	1.450
g	48	0.6	1.259	VW	1.253
h	54	1.0	1.186	m	1.183
i	66		1.072	W	1.070
j	72		1.026	VW	1.024
k	90		0.917	VW	0.917
l	98		0.878	f	0.878
m	101		0.861	f	0.861

It will be noted that the calculated value of the parameter has changed from 8.697Å in the 20% Al specimen to 8.714Å in the 40% Al specimen. This latter value is comparatively high, but it will be remembered that Cu_9Al_4 is a non-equilibrium phase in this specimen and so may possibly contain aluminium in solid solution.

No evidence of the formation of CuAl has been found at any time in these investigations.

The anomaly of the copper-aluminium system is that whereas differential thermal analysis methods indicate that the compound CuAl forms first, the X-ray data appear to show clearly that $CuAl_2$ forms first, with a subsequent transformation into Cu_9Al_4 in copper rich specimens.

Thus it appears that a comparatively low melting compound with a tetragonal structure is first formed. The electron concentration at which this phase exists is 2.33 and is very considerably greater than is the case in any of the preceding systems. The γ phase appears to form very quickly after $CuAl_2$, and to be very stable. Either this phase or Cu_3Al would have been expected to form first after a consideration of the results forthe previous systems and an inspection of the copper- aluminium diagram.

However, some other factor, or factors must operate in this case resulting in the prior formation of $CuAl_2$. Copper and aluminium are further apart in the electrochemical series than any of the previously mentioned pairs of elements so giving a greater electrochemical factor in this system. This may be partly responsible for the difference in the results obtained.

TABLE VIII.

Interplanar spacings observed in a 40%Al specimen annealed at 560°C.

Line No.	Aluminium f. c. c. I/I_1	d	$CuAl_2$ Tetragonal I/I_1	d	Cu_9Al_4 γbrass structure I/I_1	d	Observed spacings I	d	Reflections $CuAl_2$ h	k	l
a			0.484	4.28			m	4.24	1	1	0
b					0.7	3.56	W	3.5			
c			0.220	3.06			W	3.04	2.	0	0
d					0.7	2.90	VW	2.89			
e	1.0	2.33	0.462	2.37	0.6	2.32	m	2.37	2	1	1
f			0.726	2.12			W	2.13	2	2	0
g					0.4	2.11	m	2.11			
h					1.0	2.05	S	2.05			
i	0.9	2.025					S	2.025			
j			1.00	1.910			m	1.908	3	1	0
k					0.2	1.900	W	1.892			
l			0.094	1.612			f	1.609	2	2	2
m			0.073	1.509			f	1.500	3	1	2
n					0.8	1.453	f	1.450			
o	0.8	1.432			0.1	1.434	f	1.436			
p			0.069	1.409			f	1.406	4	1	1
q			0.091	1.393			f	1.391	2	1	3
r			0.111	1.357			VW	1.352	4	2	0

Line No.	Aluminium f.c.c. I/I1	Aluminium f.c.c. d	$CuAl_2$ Tetragonal I/I1	$CuAl_2$ Tetragonal d	Cu_9Al_4 γbrass structure I/I1	Cu_9Al_4 γbrass structure d	Observed spacings I	Observed spacings d	Reflections $CuAl_2$ h	k	l
s			0.151	1.288	0.5	1.285	VW	1.284	4	0	2
t	1.0	1.220	0.158	1.232	0.5	1.232	VW	1.228	3	3	2
u			0.090	1.187	1.0	1.186	W	1.184	4	2	2
v	0.5	1.169	0.027	1.172			VW	1.170	1	0	4
w			0.130	1.071		1.072	f	1.069	4	4	0
x			0.047	1.060			f	1.055	2	2	4
y			0.045	1.042			f	1.036	5	3	0
z			0.137	1.030		1.026	VW	1.026	3	1	4
aa	0.7	0.929				0.917	f	0.92			
bb	0.7	0.906					f	0.904			
cc						0.891	f	0.891			
dd	0.6	0.779					W	0.778			
ee						0.774	f	0.774			

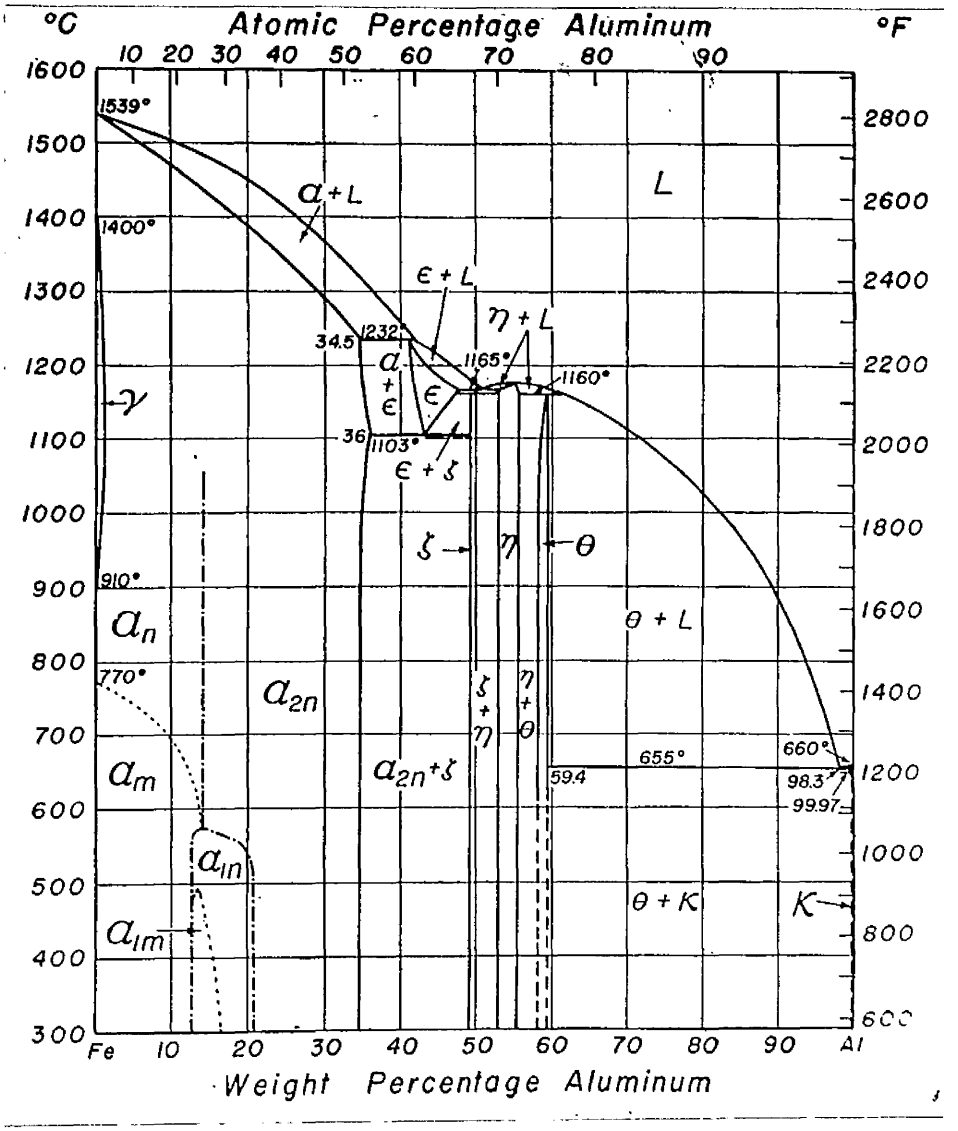

FIG. 12; IRON - ALUMINIUM EQUILIBRIUM DIAGRAM.

There is therefore a possibility that similar results would be obtained in other related systems involving aluminium.

IRON-ALUMINIUM.

In this system the electrochemical factor, though not so great as in copper-aluminium, is again higher than it was in either of the systems involving zinc. As can be seen in Fig.12 (35), the compound $FeAl_3$ forms a eutectic with Al as does $CuAl_2$. Like $CuAl_2$ it does not have a congruent melting point, though it is stable to a much higher temperature. These two compounds, though belonging to different crystal systems ($Fe Al_3$ is orthorhombic(36)) form a ternary compound on the join between them, $Cu_2 Fe Al_7$ or $2CuAl_2 FeAl_3$ which is also tetragonal.

The compound Fe_2Al_5 has recently been shown by Schubert and Kluge(37) to show similarities with $CuAl_2$ in bonding and electron configuration. As in the copper-aluminium system a phase, FeAl, appears at an electron concentration of 1.5, provided that iron be considered to have zero valency. According to Hume-Rothery and Coles,(38) it is possible, however, that iron may in fact show a negative valency, though not necessarily of the order suggested by Raynor. For this reason electron concentration values cannot be stated for this system with the same certainty as for the systems considered earlier. This same condition may also apply to some systems containing nickel, though it is probable that in zinc, nickel has zero valency.

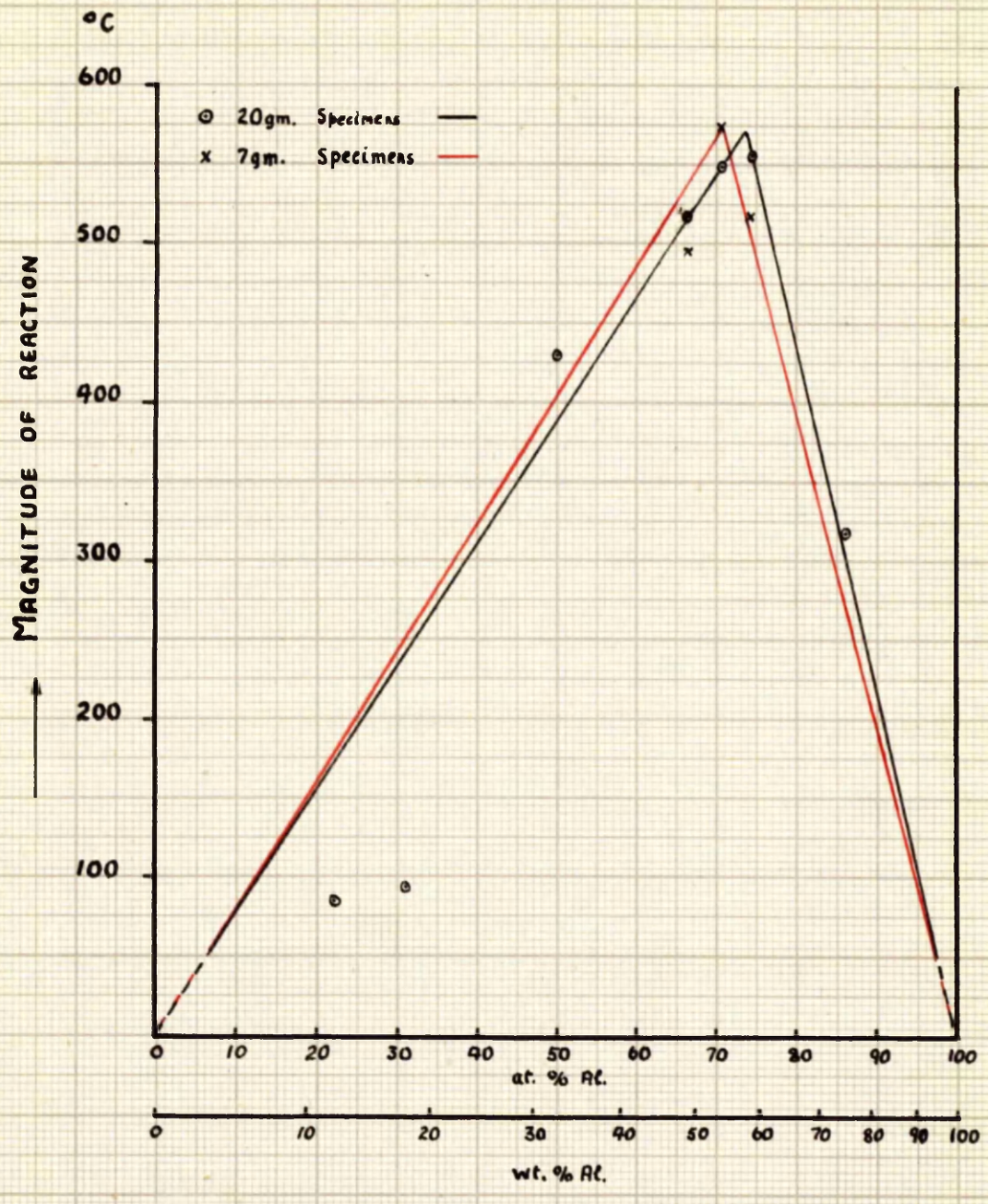

FIG. 13; VARIATION OF THE MAGNITUDE OF THE EXOTHERMIC REACTION WITH THE COMPOSITION OF THE COMPACT IN THE IRON–ALUMINIUM SYSTEM.

If iron be given zero valency when alloyed with aluminium, the $FeAl_3$ compound would have an electron concentration of 2.25 which is of the same order as in $CuAl_2$.

In view of these similarities with copper-aluminium it was decided to investigate the progress of sintering in this system.

Differential Thermal Analysis.

The results of a series of differential thermal analysis experiments are shown in Table IX and in Fig.13. the magnitudes of the observed heat charges are plotted against the composition of the compact. It will be seen that the results for the compacts containing 54% and 58% Al are very close together, in one case the 58% Al specimen, corresponding to $FeAl_3$ giving a slightly higher reading than the 54% Al specimen, which is in the Fe_2Al_5 field. It was feared that with large specimens there might be an error of up to 30°C in the maximum temperature recorded during the exothermic change. In order to reduce this and differentiate more clearly between these compositions specimens of only 7 grammes in weight were prepared. These gave reproducible results showing that the highest readings were obtained with compacts containing 54% Al, (the composition corresponding to Fe_2Al_5).

As will be seen from Fig.13, the change appears to have been more accurately recorded, as the points are a better fit for the graph than is the case with the large specimens. It will be seen that the magnitude of the exothermic reaction recorded in the Fe_2Al_5 and $FeAl_3$ specimens (550C°) is of the same order as the value obtained by extrapolation in

TABLE IX.

Differential Thermal Analysis of Iron-Aluminium Compacts.

Composition Fe	Al	Corresponding Compound.	Reaction Temperature °C	Magnitude of Exothermic Change °C.
(a) 20 gm. specimens.				
88	12	Fe_3Al	565 685	38 46
82	18	-	556 698	61 31
68	32	Fe Al	565	431
51	49	Fe Al_3	568	517
46	54	Fe_2Al_5	570	548
42	58	Fe Al_3	564	556
25	75	-	570	318
(b) 7 gm. specimens.				
51	49	$FeAl_3$	575	493
46	54	Fe_2Al_5	573	575
42	58	$FeAl_3$	540	517
25	75	-	562	277

TABLE X.

Structure observed during the Sintering of several Iron-Aluminium Alloys.

(a) 12% Al (Composition of Fe_3Al)

Temp. °C.	Time hrs.	Iron	FeAl	$FeAl_2$	Fe_2Al_5	$FeAl_3$	Aluminium
450	62	Strong	-	-	V.Weak	-	-
500	69	Strong	-	-	Weak	-	-
550	61	Strong	-	-	Weak	V.Weak	-
600	66	Strong	-	Faint	Weak	Faint	-
650	69	Strong	-	Trace	V.Weak	poss.trace	-
750	62	Strong	Strong	-	-	-	-

(b) 32% Al (Composition of FeAl).

Temp. °C.	Time hrs.	Iron	FeAl	$FeAl_2$	Fe_2Al_5	$FeAl_3$	Aluminium
450	62	Strong	-	Trace	Weak	-	Medium
500	69	Medium	-	V.Weak	Medium	Trace	-
550	61	Weak	Weak x	Faint	Weak	V.Weak	-
600	66	Faint	Medium *	Faint	Weak	Faint	-
650	69	-	Strong *	Faint	Weak	-	-
750	62	-	Strong	-	Trace	-	-

(c) 49% Al (Composition of $FeAl_2$)

Temp. °C.	Time hrs.	Iron	FeAl	$FeAl_2$	Fe_2Al_5	$FeAl_3$	Aluminium
450	62	Strong	-	-	Weak	Trace	Medium
500	69	Strong	-	-	Medium	Faint	Medium
550	61	Trace	-	V.Weak	Strong	Weak	-
600	66	Trace	-	Weak	Strong	Weak	-
1000	96	-	-	Strong	Weak	V.Weak	-

x Disordered * Partially ordered.

(d) 54% Al (Composition of Fe_2Al_5).

Temp. °C	Time hrs.	Iron	FeAl	$FeAl_2$	Fe_2Al_5	$FeAl_6$	Aluminium
425	90	Strong	-	-	-	-	Strong
450	62	Strong	-	-	V.Weak	Faint	Strong
550	69	V.Weak	Faint	Faint	Strong	V.Weak	V.Weak
600	66	-	Faint	Faint	Strong	V.Weak	-
1000	96		-	-	Strong	Faint	-

(e) 58% Al (Composition of $FeAl_3$)

Temp. °C.	Time hrs.	Iron	FeAl	$FeAl_2$	Fe_2Al_5	$FeAl_3$	Aluminium
425	90	Strong	-	-	V.Weak	-	Strong
450	62	Strong	-	-	V.Weak	Faint	Strong
500	69	Medium	-	-	Weak	Weak	Medium
550	61	-	Trace	-	Strong	Weak	-
600	66	-	-	-	Strong	Medium	-
1000	96	-	-	-	Strong	Weak	-

(f) 75% Al (in field $FeAl_3$ + Al)

Temp. °C	Time Hrs.	Iron	FeAl	$FeAl_2$	Fe_2Al_5	$FeAl_6$	Aluminium
500	69	Weak	-	-	Weak	V.Weak	Strong
600	66	-	-	-	Medium	Weak	Medium
650	69	-	-	-	Medium	Medium	Medium

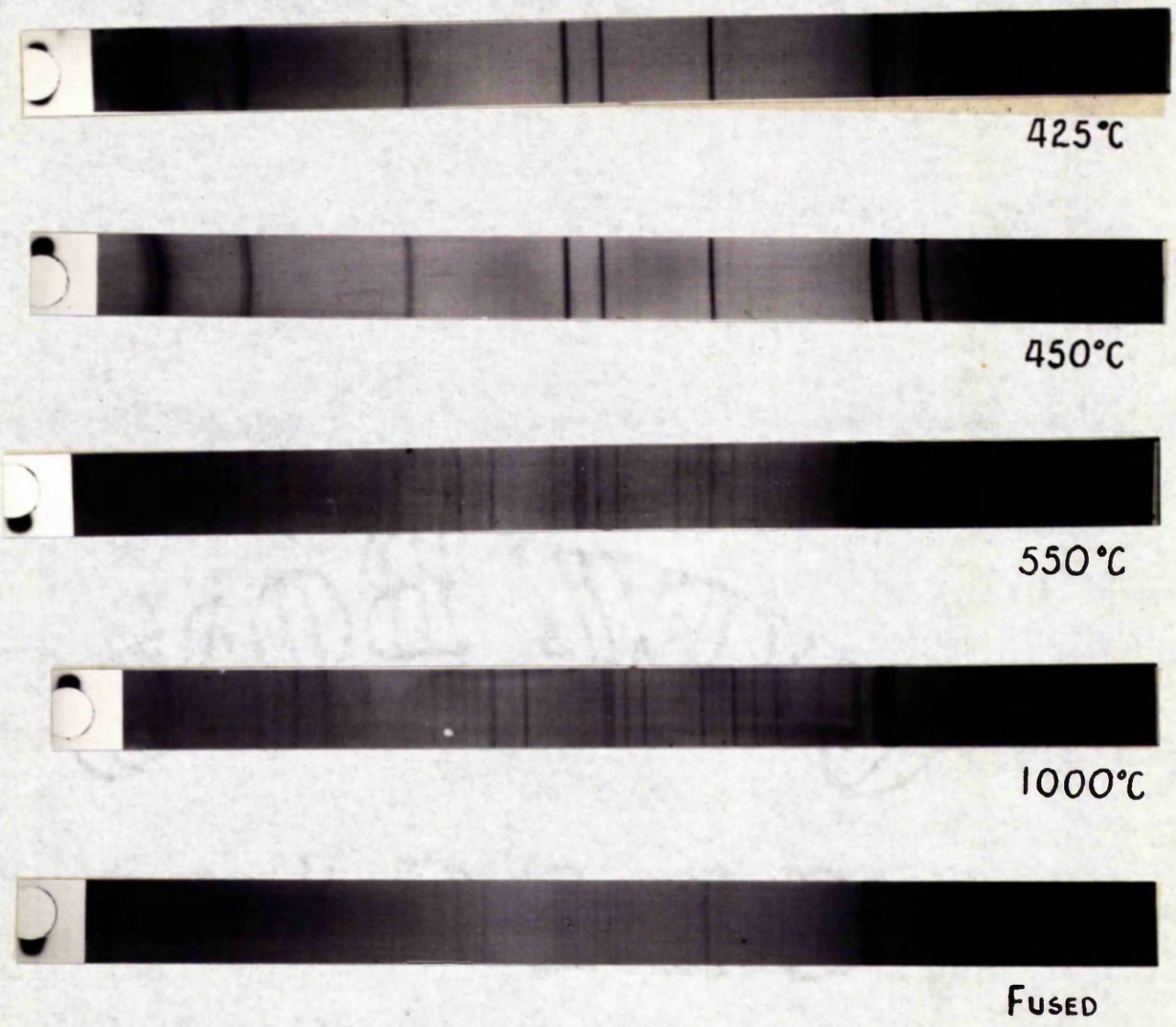

FIG. 14 a); X-RAY PHOTOGRAPHS OF IRON - ALUMINIUM SPECIMENS CONTAINING 58% AL. ANNEALED AT VARIOUS TEMPERATURES.

Fig.8. This is the value which might have been recorded by $CuAl_2$ had there been no liquid formation.

Differential thermal analysis has indicated that a compound in the region 54 - 60% Al is the first to form. It appears probable that the compound is Fe_2Al_5. More conclusive evidence, however, must be sought by X-ray examination.

X-ray Crystallographic analysis.

The results of a series of X-ray examinations are shown in Table X and in Fig.14. The compositions chosen represent the various iron-aluminium compounds. The sintering time was normally kept constant at 60-65 hours. Fig.14 illustrates the progress of sintering of most of the iron-aluminium compounds with increase in annealing temperatures, and is composed of some of the powder photographs used to derive Table X.

The lowest temperature at which compound formation was observed was 425°C. The specimen used here had previously been sintered for 70 hours at 400°C without sign of any lines other than those of iron and aluminium. In Fig.14a, the first film had lines belonging to iron and aluminium but has also 5 other weak or faint lines. Two of these lines can only belong to Fe_2Al_5. Another two are the strongest lines of Fe_2Al_5 but could also be said to belong to $FeAl_3$ which has medium strength lines at these angles. The fifth line can be represented by a weak strength Fe_2Al_5 line or by a weak FeAl line. The strongest lines of $FeAl_3$ and of FeAl are not observed. It is concluded from this that Fe_2Al_5 is the compound present, and so is the compound to be formed first. The curious point is that although

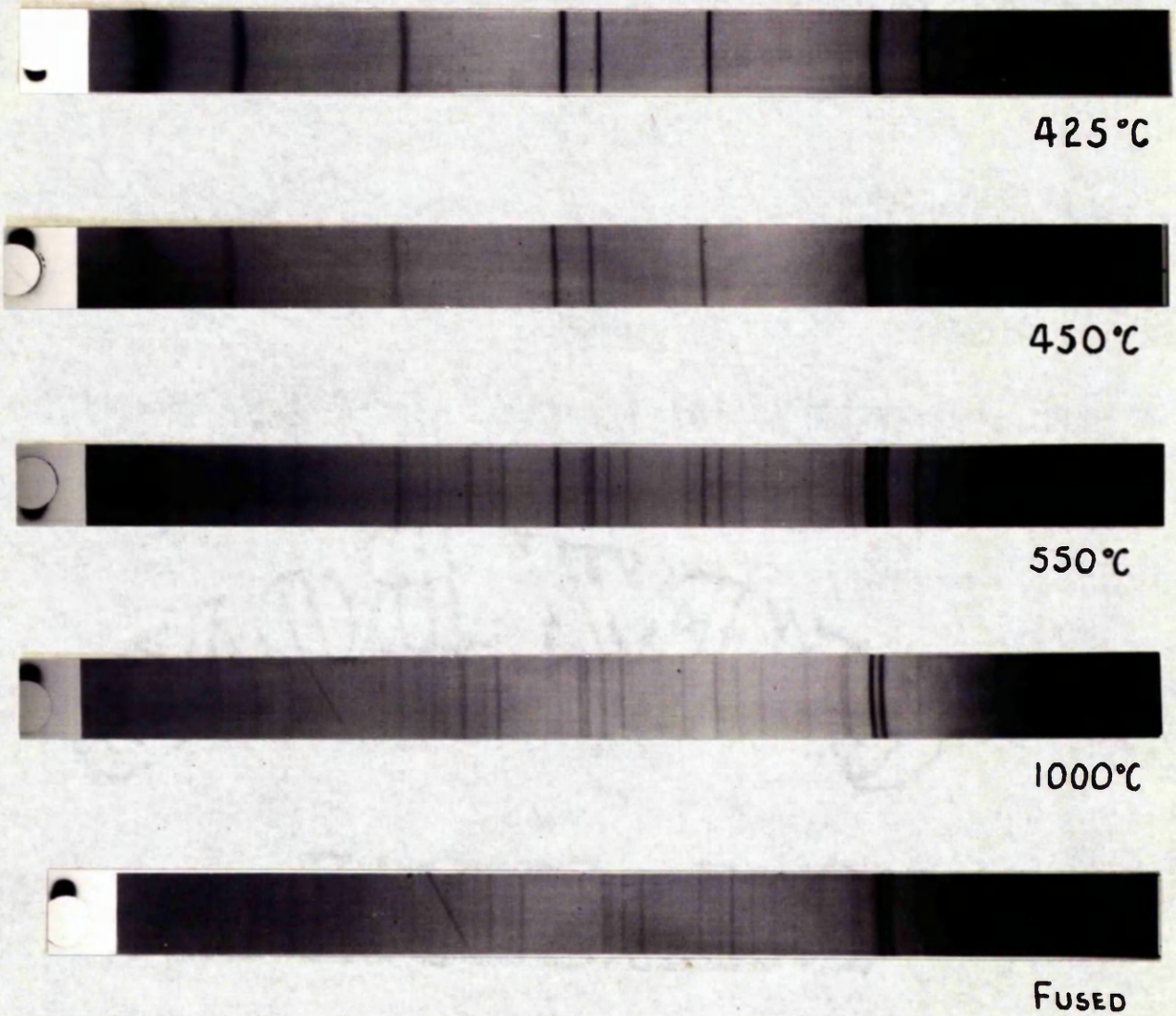

FIG. 14b); X-RAY PHOTOGRAPHS OF IRON - ALUMINIUM SPECIMENS CONTAINING 54% AL. ANNEALED AT VARIOUS TEMPERATURES.

this compound formation is found in the 58% Al specimen, none is found in the 54% Al specimen at the composition of Fe_2Al_5, as can been seen in Fig.14b.

By 450°C compound formation can be observed in all the compositions investigated. In all but the iron-rich specimens both Fe_2Al_5 and $FeAl_3$ are found, lines characteristic of the former always being present in greater intensity. As the sintering temperature is raised the initial reaction proceeds to completion and the lines of iron and aluminium disappear. Those of aluminium tend to disappear earlier than those of iron due to the lower scattering power of the aluminium atom.

By 500-550°C the initial reaction is complete and the second stage of homogenisation is beginning. Thus in the case of the 32% Al specimen at 550°C $FeAl_3$ and FeAl exist in addition to the Fe_2Al_5, $FeAl_3$ and iron, indicating diffusion gradients between the initial centres of compound formation and the remaining iron. Fig.14c, illustrates the complex appearance of the X-ray structures at this stage. Similar structures are found in the other specimens at this temperature.

When the sintering temperature is raised to 750°C the iron rich specimens are almost completely homogeneous though there is little alteration in the observed structures of the three compositions between 50-60% Al. The specimen containing 32% Al, shows the ordered structure of FeAl at this temperature as is seen in Fig.14c, only a trace of Fe_2Al_5 remaining. The observed interplanar spacings are given in Table XI, in which are also given the corresponding reflections on the A.S.T.M. Card for FeAl. The lattice

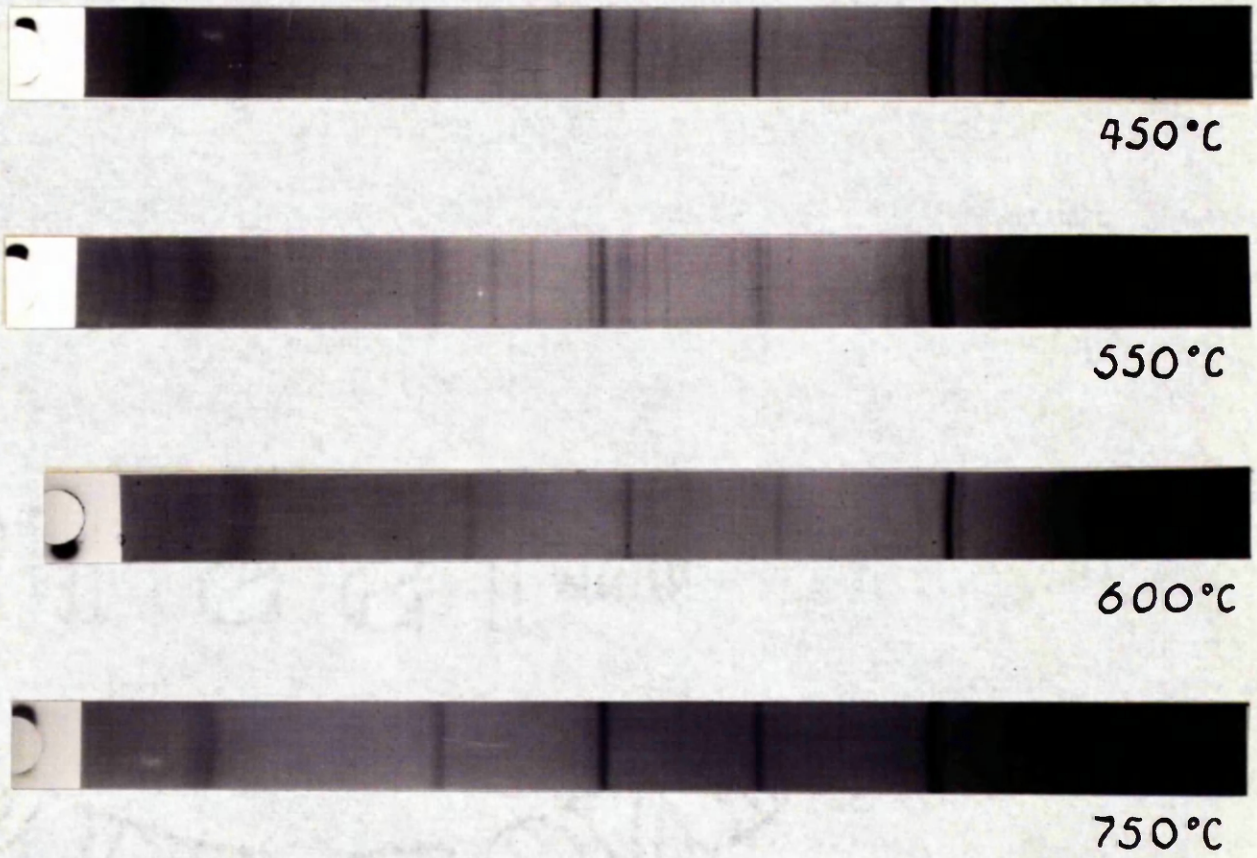

FIG. 14c); X-RAY PHOTOGRAPHS OF IRON - ALUMINIUM SPECIMENS CONTAINING 32% AL. ANNEALED AT VARIOUS TEMPERATURES.

constant derived from the observed lines of FeAl is a = 2.904Å. This is in good agreement with the value given by Taylor(36) a = 2.903Å. The 12% Al specimen at this temperature shows a mixture of unalloyed iron and FeAl indicating that it too has reached equilibrium.

After 100 hours at 1000°C the 49% and 54% Al specimens showed a greater degree of homogenisation in contrast to the 58% Al specimen which appeared to have less $FeAl_3$. Chemical analysis showed that while the compositions of the first two specimens had not altered appreciably the composition of the third specimen was now 56% Al, and as such the X-ray diagram was probably comparable with the others, in indicating how close the structure was to equilibrium.

Attempts to anneal specimens of these compositions at 1150°C, i.e., just under the melting points of the compounds, had to be discontinued when it was found that almost half the aluminium was lost by volatilisation during sintering for 60 hours. Calculations showed that at this temperature the vapour pressure of aluminium was about one-third of the pressure in the vacuum tube, so making possible such a large loss of aluminium.

Specimens corresponding to these three compounds were prepared by melting in a high frequency furnace, in a carbon monoxide atmosphere, 2 minutes being allowed for melting. Subsequently they were annealed at 1000°C for 50 hours. Their compositions on analysis were 45%, 56% and 61% Al. The observed interplanar spacings, and where practicable their indices are recorded in Table XII, section (a) for the 45% Al specimen, section (b) for the 56% Al specimen and section (c) for the 61% Al specimen. The first specimen falls in the region FeAl + $FeAl_3$ of the equilibrium diagram. This is the reason for the return of the strong cubic pattern

TABLE XI.

Reflexions from 32% Al specimen sintered at 750°C.

N	FeAl Card CsCl Structure.		Observed spacings.		Reflexions.		
	I/I_1	d(Å)	I	d(Å)	h	k	l
1	0.12	2.89	W	2.91	1	0	0
	Fe_3Al_5	-	f	2.106			
2	1.00	2.04	V.S.	2.054	1	1	0
3	0.04	1.673	f	1.675	1	1	1
4	0.08	1.448	S	1.449	2	0	0
5	0.03	1.298	f	1.299	2	1	0
6	0.20	1.182	S	1.182	2	1	1
	Analloyed iron		f	1.167			
8	0.02	1.027	S	1.025	2	2	0
10	0.02	0.917	S	0.920	2	2	1

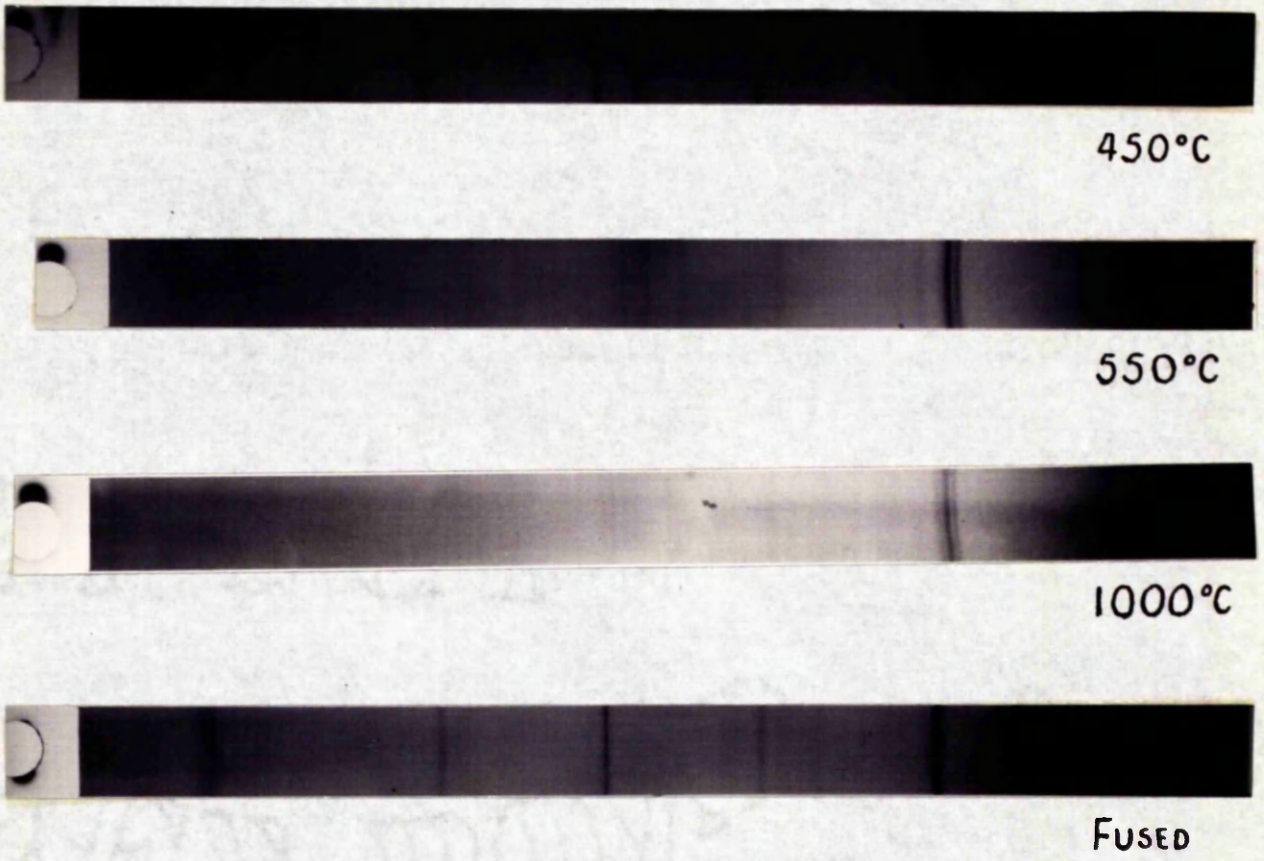

FIG. 14 d); X-RAY PHOTOGRAPHS OF IRON - ALUMINIUM SPECIMENS CONTAINING 49% AL. ANNEALED AT VARIOUS TEMPERATURES.

which can be seen in Fig.14 d. The remaining lines belong to $FeAl_2$ with the exception of two lines (h, j) which may belong to Fe_2Al_5. The strongest Fe_2Al_5 lines, which have not been observed could be masked by $FeAl_2$ lines. As no A.S.T.M. Card existed for $FeAl_2$ a table of possible values of $\sin^2\theta$ was computed from the published parameters of $FeAl_2$ (36). This gave all the possible reflections for this structure. Values of $\sin^2\theta$ were calculated for the observed lines and these values compared with those in the Table. This also enabled the observed lines to be indexed. Also shown in section (a) of Table XII, are the interplanar spacings derived from the calculated $\sin^2\theta$ values. It will be seen that a close correlation is achieved. As an additional check, the experimental results were further analysed. Using the experimental results and the indices obtained in the previous comparisons the parameters of the rhombohedral structure were derived. They were found to be $a = 6.325\text{Å}$, $\alpha = 74°9'$, the published values being $a = 6.326\text{Å}$, $\alpha = 74°9'$ (36).

The second of the fused alloys lies at the aluminium rich side of the Fe_2Al_5 phase field. The presence of some faint FeAl and $FeAl_3$ lines, shown in Fig.14b and Table XIIb, seem to indicate that equilibrium has not yet been reached. The Table gives a comparison of the observed interplanar spacings with those of FeAl, Fe_2Al_5 and $FeAl_3$ as given by the A.S.T.M. Cards. Lines w, and ai, have been observed in many specimens which contain $FeAl_3$ though they have not been indexed in the Table of $\sin^2\theta$ for $FeAl_3$, which is described later. In view of the close agreement between the experimental values and those from the Card, the calculation

TABLE XII.

Reflexions Observed in Fused Alloys.

(a) 45% Al.

Line No.	FeAl Card. CsCl structure.		$FeAl_3$ calculated rhombohedral.	Observed Spacings.		Reflexions ($FeAl_3$)		
	I/I_1	d(Å)	d(Å)	I	d(Å)	h	k	l
a			3.4	f	3.47	0	0	4
b	0.12	2.89		w	2.91			
c			2.54	vw	2.54	1	1	4
d			2.09	w	2.09	3	0	2
e	1.00	2.04		vs	2.057			
f			2.01	vw	2.011	2	1	4
g			1.832	f	1.827	3	1	0
h	Fe_2Al_5			f	1.734			
i	0.04	1.673		f	1.681			
j	Fe_2Al_5			vw	1.597			
k			1.507	f	1.509	3	2	1
l	0.03	1.448	1.460	w	1.452	2	2	6
m			1.408	f	1.402	2	1	8
n			1.374	f	1.370	4	1	3
o	0.03	1.298		f	1.300			
p			1.266	f	1.260	3	3	1
q			1.239	f	1.235	0	0	11
r			1.217	f	1.214	4	1	6
s	0.2	1.182	1.184	m	1.185	2	2	9
t			1.092	f	1.095	3	1	10
u			1.080	f	1.077	3	0	11
v	0.02	1.027	1.030	w	1.028	5	2	3
w	0.02	0.917		w	0.920			

(b) 56% Al.

Line No.	Fe Al Card Cs Cl Structure.		Fe_3Al_5 Card Orthorhombic		$FeAl_3$ Card. Orthorhombic		Observed Spacings.	
	I/I_1	d(Å)	I/I_1	d(Å)	I/I_1	d(Å)	I	d(A)
a			0.24	3.86	0.4	3.95	f	3.83
b			0.4	3.2	0.2	3.33	w	3.20
c						2.48	f	2.49
d			0.1	2.39	0.6	2.34	f	2.36
e					0.4	2.25	f	2.25
f			1.0	2.11			s	2.116
g			1.0	2.05			s	2.059
h					1.0	2.02	f	2.00
i					0.2	1.987	f	1.971
j			0.1	1.94	0.4	1.936	vw	1.936
k			0.08	1.90	0.2	1.910	vw	1.908
l			0.08	1.76			f	1.760
m	0.04	1.673					f	1.662
n			0.03	1.593			f	1.599
o		0	0.1	1.523			vw	1.527
p			0.16	1.478			w	1.470
q	0.08	1.448			0.6	1.434	f	1.439
r			0.02	1.421			f	1.419
s			0.1	1.393			vw	1.391
t			0.1	1.275			w	1.271
u			0.08	1.242			w	1.240
v			0.16	1.214			w	1.219
w					$FeAl_5$		vw	1.210
x	0.2	1.182	0.02	1.182			f	1.175
y			0.08	1.104			w	1.103
z			0.02	1.092			f	1.090
aa			0.1	1.070			w	1.070
ab					0.4	1.063	vw	1.057
ac						1.045	vw	1.044
ad			0.03	1.033			vw	1.034
ae			0.02	1.020			f	1.019
af		iron					f	1.005
ag						0.955	vw	0.952
ah					$FeAl_6$		w	0.941
ai						0.934	vw	0.931
aj						0.928	f	0.925

(c) 61% Al.

Line No.	$FeAl_3$ Calculated.	Orthorhombic Card.		Observed Spacings.		Roflexions ($FeAl_2$)		
	d(Å)	I/I_1	d(Å)	I	d(Å)	h	k	l
a		0.4	3.95	vw	3.99	3	5	1
b		0.6	3.68	w	3.66	5	5	1
c		0.6	3.54	w	3.53	1	1	3
d		0.2	3.33	vw	3.33	7	1	3
e		0.2	3.26	vw	3.25	6	6	0
f	2.54			vw	2.53	6	2	4
g	2.46			vw	2.45	8	8	0
h		0.1	2.36	vw	2.36	4	4	4
i		0.6	2.34	vw	2.30	6	4	4
j		0.4	2.25	vw	2.25	5	7	3
k		0.1	2.16	f	2.16	9	9	1
l		1.0	2.09	s	2.086	7	1	5
m		1.0	2.04	s	2.033	5	3	5
n		1.0	2.02	s	2.012	10	6	4
o		0.2	1.987	f	1.974	9	5	3
p		0.4	1.936	f	1.932	3	9	3
q	1.489			f	1.490	7	3	7
r	1.467			f	1.465	6	8	6
s		0.6	1.451	w	1.440	1	5	7
t		0.4	1.348	f	1.341	4	0	8
u	1.306			f	1.303	8	4	8
v		0.6	1.293	f	1.286		-	
w	1.261			vw	1.259	0	6	8
x		0.3	1.252	f	1.248	6	6	8
y		0.4	1.227	vw	1.225	10	6	8
z				vw	1.210		-	
aa	1.199			vw	1.198	0	8	8
ab		0.4	1.182	vw	1.177	3	3	9
ac		0.1	1.171	f	1.167	9	3	9
ad		0.1	1.129	f	1.122	6	10	8
ae		0.4	1.091	vw	1.086		-	
af	1.080			f	1.077	4	0	10
ag	1.067			f	1.070	6	2	10
ah		0.4	1.068	vw	1.061	5	9	9

was carried no further. The published parameters for this phase, which is orthorhombic, are a = 7.68; b = 6.40; c = 4.20Å (39).

The last of the fused alloys lies slightly to the aluminium side of $FeAl_3$. However, no aluminium lines are observed only those of $FeAl_3$ being found as is seen in Fig.14a and Table XIIc.

The table gives the observed spacings plus the spacings and intensities on the corresponding A.S.T.M. Card. Because this Card is incomplete a Table of $\sin^2\theta$ values was computed in a manner similar to that for $FeAl_3$. This enabled the observed lines to be indexed. Where no value was given on the A.S.T.M. Card the corresponding "d" value was calculated from the $\sin^2\theta$ value, and is shown in Table XIIc. Even after this had been done line Z remained unaccounted for. This line has been found in all 58% Al specimens containing appreciable amounts of $FeAl_3$ and also in some 54% Al specimens, including the fused alloy in Table XIIb (line w). In addition two lines which are given on the A.S.T.M. Card were not able to be indexed. It is presumed that the value of either h or k for these lines is greater than 10, the highest value in the Table. The parameters used in this calculation were obtained from Taylor(36), the original work being by Bachmetev(40). This shows $FeAl_3$ to have an orthorhombic structure, a = 15.49Å, b = 8.11Å, c = 47.6Å.

Recently Black(41) has shown that $FeAl_3$ is monoclinic in structure with the following lattice constants; a = 15.489Å, b = 8.0331Å, c = 12.476Å, $\beta = 107°43'$. Since the size of this unit cell is approximately 1/3 of the earlier one and many possible reflections in the calculation were not observed, it is probable that the correlation

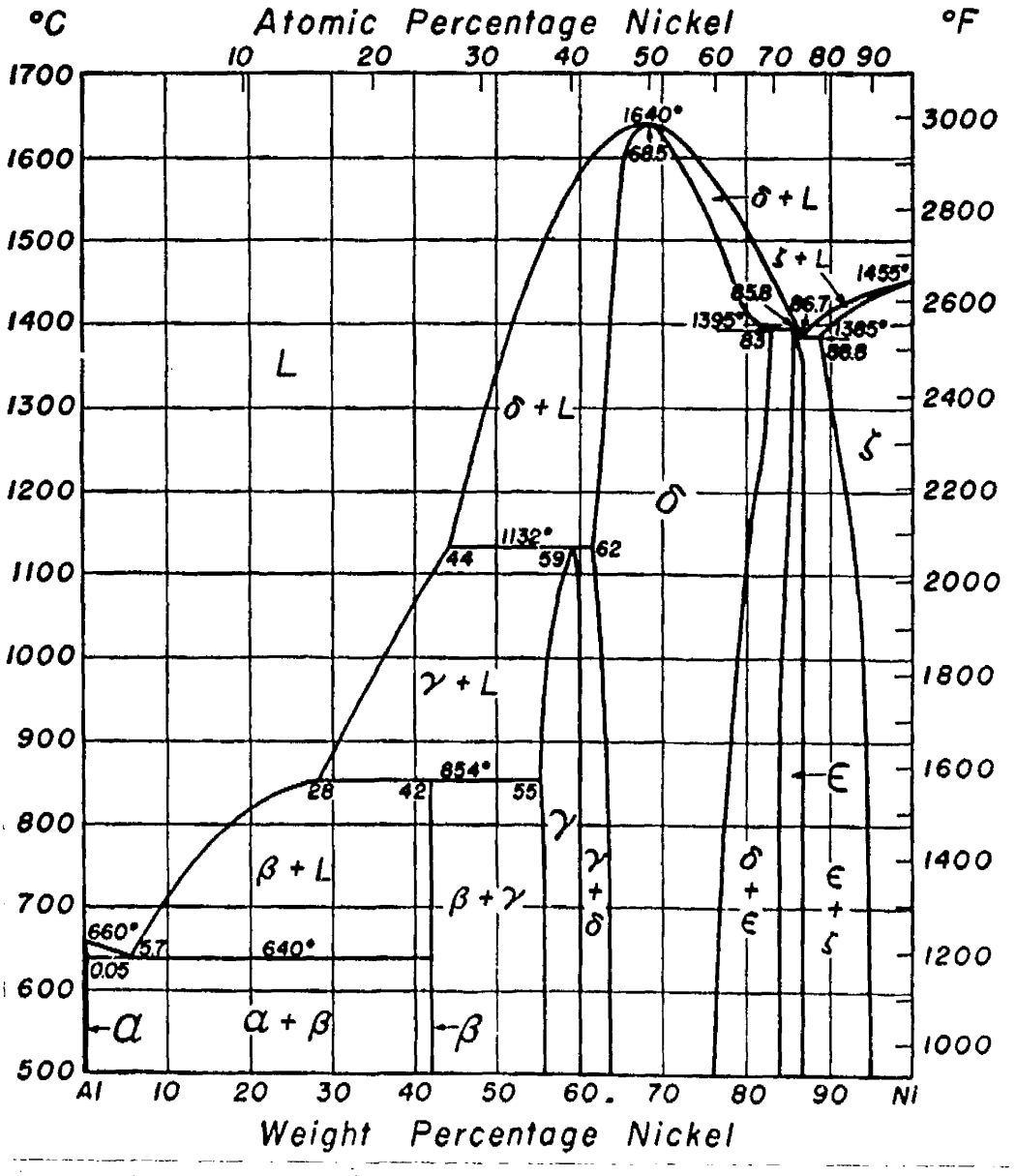

FIG.15; NICKEL - ALUMINIUM EQUILIBRIUM DIAGRAM.

obtained between the observed and calculated "d" values is correct, though it is improbable that the indices are correct.

From these results it can be seen that Fe_2Al_5 is the first compound to form, though $FeAl_3$ forms very quickly after it, at almost all compositions. The superlattice structure FeAl does not appear until an advanced state of homogenisation has been reached.

Thus the process of compound formation is somewhat similar to that in copper-aluminium in that a phase rich in aluminium forms first. Here, however, it is not the phase richest in aluminium but the one next to it which possesses a congruent melting point and so possibly a stronger state of interatomic bonding. Judging from the appearance of these two phases ($FeAl_3$ and Fe_2Al_5) in the diagram, they are fairly similar as regards stability. However, Fe_2Al_5 has the higher heat of formation and also a congruent melting point. These factors may be sufficient to swing the balance in its favour.

In view of the support given by the results of the iron-aluminium system to those of copper-aluminium it was decided to investigate the system nickel-aluminium.

NICKEL-ALUMINIUM.

As can be seen from Fig.15(42), this system shows considerable similarity to the iron-aluminium system. The greatest dissimilarity is in the relative stabilities of the different compounds, particularly in the NiAl phase.

NiAl has a body centred cubic structure. It has the high

congruent melting point of 1640°C and in this respect differs markedly from the other phases which form as a result of peritectic reactions. The published value of the heat of formation is 34 k.cals/mol. slightly lower than that of $NiAl_3$, which seems to be at variance with its evident stability and the apparent lower stability of $NiAl_3$.

On the other hand in the iron-aluminium system the alloy FeAl is not a separate phase but merely an ordered arrangement of the solid solution based on the iron lattice. As such it would be expected to have a relatively lower stability than NiAl. It would also be expected that its stability would be less than that of Fe_2Al_5 which has a considerably higher head of formation and is the only compound in this system with a congruent melting point.

Thus in the nickel-aluminium system there is a phase $NiAl_3$ rich in aluminium and with a structure similar to $FeAl_3$ which one might expect to form judging from the results of the other aluminium systems. There is, however, another phase NiAl, similar in structure to CuZn, which would appear to be very much more stable, and occurs at an electron concentration of about 1·5, depending on the exact valency assigned to nickel.

When a specimen containing 32% Al, corresponding to the compound NiAl, was analysed using the differential thermal technique, two exothermic heat changes were recorded. The first heat evolution corresponding to a rise of 75°C in temperature occurred at 555°C. This was followed at 694°C by a much larger evolution of heat in which a rise of 700°C was recorded on the differential thermocouple.

A specimen containing 14% Al was found to exhibit similar changes, as there was a heat evolution causing a rise in temperature of 50C° at 542°C and a further evolution of 10C° at 689°C.

Though the reason for the double heat changes could not be conclusively elucidated, it was observed that they were completely reproducible. Similar double heat changes have been observed in iron rich, iron-aluminium compacts.

X-ray analysis using back reflection methods(43) seemed to indicate the presence of both NiAl and Ni_3Al in specimens annealed and quenched from 500°C.

A series of nickel-aluminium compacts made up to compositions differing, one from another by 10% were annealed at 800°C for a short period. On examination it was found that the compact containing 30% Al was in a semi-fused condition while those on either side were greatly swollen. The amount of growth appeared to decrease the further the composition of the compact was from 30% Al. It would appear that during annealing an exothermic reaction had taken place, the magnitude of which varied with the composition of the compact, and reached a maximum in that with 30% Al. This would seem to agree with the differential thermal analysis results in pointing to NiAl as the compound which is formed first.

In this system the tendency present in the other aluminium systems, for an aluminium rich phase to form first appears to be counteracted by the much greater stability of the NiAl phase.

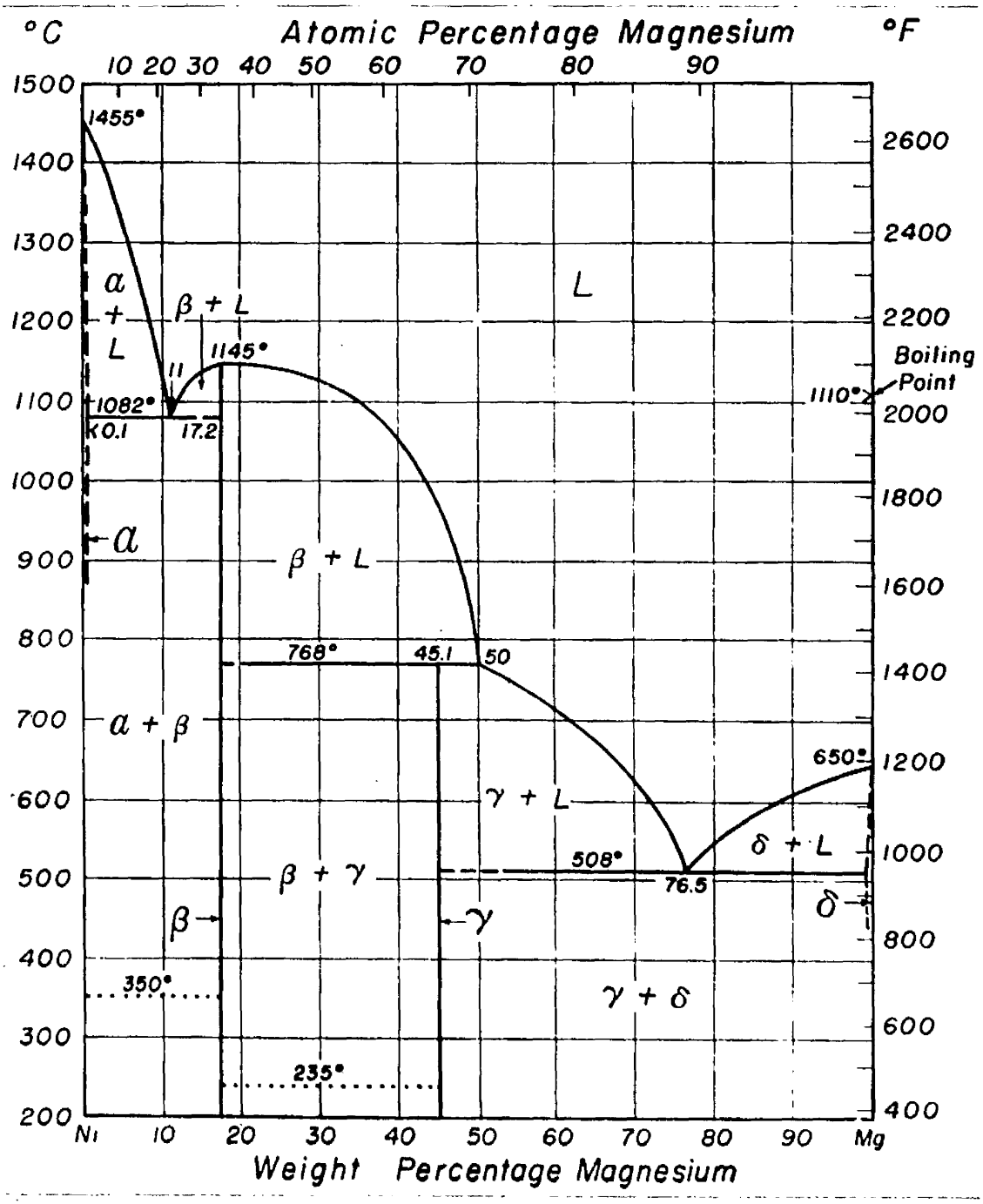

FIG. 16; NICKEL - MAGNESIUM EQUILIBRIUM DIAGRAM.

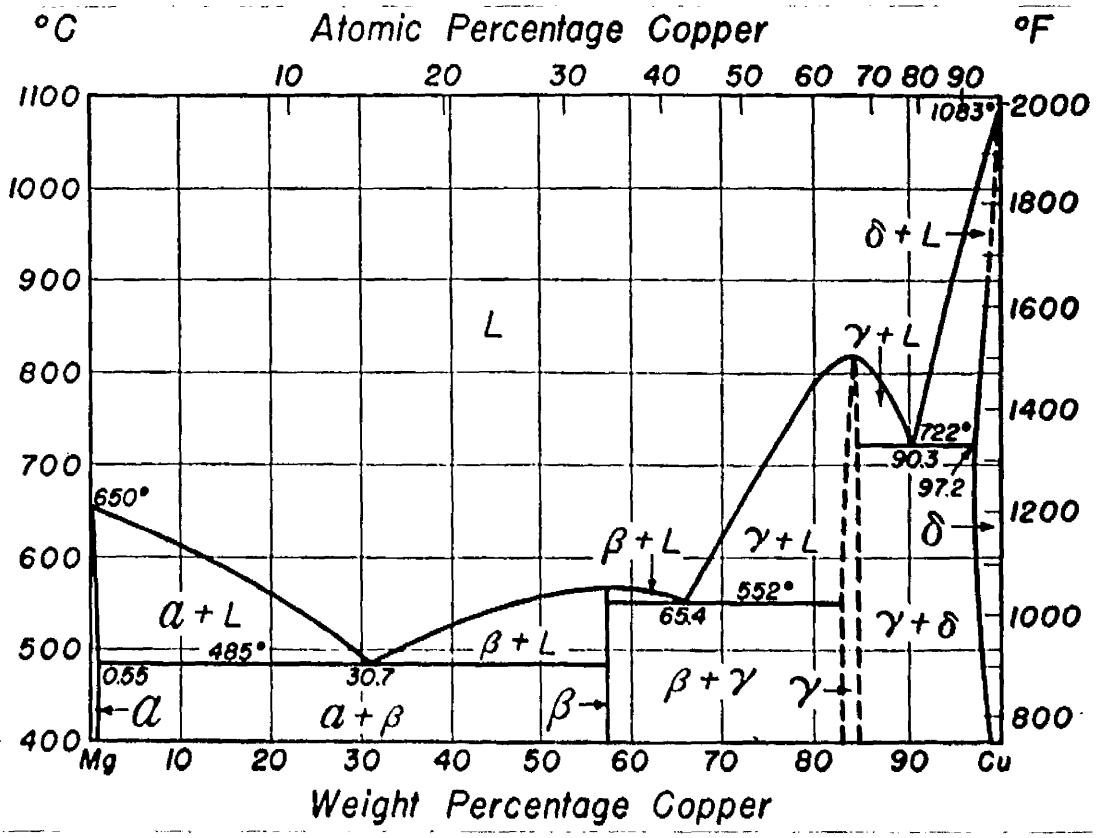

FIG. 17: COPPER - MAGNESIUM EQUILIBRIUM DIAGRAM.

In general, therefore, it appears to be the compound with the greatest stability which forms first. This stability may be indicated by a congruent melting point, also by a high temperature stability and a high heat of formation, both of which may be greater than for any other compound in the system. However, if there is a compound with a structure similar to that of $CuAl_2$ there is a tendency for this to form, provided the other factors do not outweigh it.

NICKEL-MAGNESIUM AND COPPER-MAGNESIUM.

These two systems have very similar equilibrium diagrams as can be seen in Figs.16 and 17 (44 and 45), there being two compounds in each case, M_2Mg and MMg_2.

The M_2Mg compound appears in each system to be the more stable as it is the higher melting of the two and has a congruent melting point. Ni_2Mg is hexagonal while Cu_2Mg is face centred cubic.

Similarly the two MMg_2 compounds are homotypes and are likewise related to the structure of $CuAl_2$. $CuMg_2$ is orthorhombic, face centred, while $NiMg_2$ is hexagonal(46). $CuMg_2$, it will be seen, has a congruent melting point but $NiMg_2$ is formed as a result of a peritectic reaction.

The heats of formation of all four compounds are very close, all being in the range 22.0 - 23.7 k.cals/mol. These values give no apparent indication of the relative stabilities of the compounds. The electro-chemical factor in both systems is again high, being of the same order as for iron-aluminium and copper-aluminium.

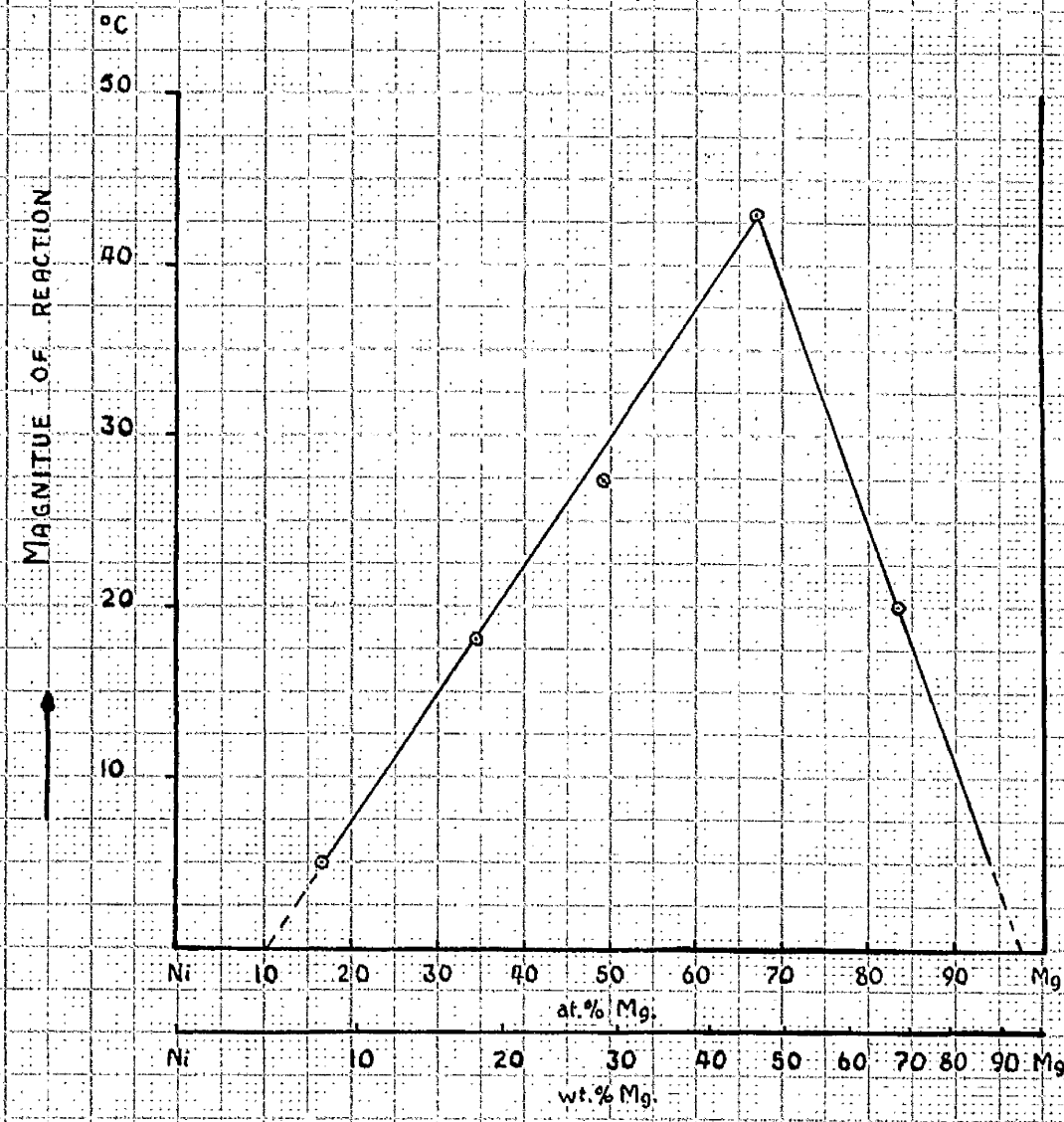

FIG. 18; VARIATION OF THE MAGNITUDE OF THE EXOTHERMIC REACTION WITH COMPOSITION IN THE NICKEL – MAGNESIUM SYSTEM.

In each system, therefore, the compound which forms is either one which is stable to a relatively high temperature with a congruent melting point and having a low electron concentration, or one which has a lower melting point (only in one case congruently melting) and a higher electron concentration but which has a structure similar to that of $CuAl_2$.

TABLE XIII.

Differential Thermal Analysis of Nickel-Magnesium Compacts.

Composition Ni	Mg	Compound to which stated composition corresponds.	Reaction Temperature °C.	Magnitude of Exothermic Change C°.
92.5	7.5	-	467	5
83	17	Ni_3Mg	440	18
71	29	-	436	27
55	45	$NiMg_2$	435	43
32	68	-	442	20

Table XIII contains the results of a number of experiments in the nickel-magnesium system, using differential thermal analysis. The magnitudes of the exothermic changes are plotted against composition of the compact in Fig. 18. It will be seen that the greatest heat evolution occurs in the 45% Mg compact corresponding to the compound $NiMg_2$. X-ray experiments have shown that at 450°C $NiMg_2$ was present in all these specimens while Ni_3Mg was absent from them all(43).

Experiments with the copper-magnesium system gave very similar results (Table XIV). The largest exothermic change, as indicated by differential thermal analysis occurred in compacts containing 42% Mg, corresponding to $CuMg_2$.

TABLE XIV.

Differential Thermal Analysis of Copper-Magnesium Compacts.

Composition Cu	Mg	Compound	Reaction Temp. °C.	Magnitude of Exothermic Change C°
84	16	Cu_2Mg	485	5
72	28	-	512	10
58	42	$CuMg_2$	475	25
30	70	-	473	5

X-ray investigations confirmed these findings. The compacts were made up to one of two compositions representing the two intermetallic compounds. At the lowest annealing temperature which was just above the reaction temperature, as indicated by differential thermal analysis, lines corresponding to $CuMg_2$ appeared. Owing to the short annealing time the reaction was incomplete, as can be seen from Table XV. Copper lines were found in all the specimens except that of 42% Mg, annealed for 12 hours at 595°C. This specimen showed only $CuMg_2$. Despite the absence of lines corresponding to magnesium in the X-ray diffraction spectrum, quantities of the metal may be present in the specimens treated at the lower temperatures. The absence of diffraction lines could be accounted for by the fairly small

TABLE XV.

Structures Observed in Copper-Magnesium Compacts.

Temp. °C.	Time hrs.	Copper	Cu_2Mg	$CuMg_2$	Magnesium
(a) Specimens containing 16% Mg.					
505	1	Strong	-	Faint	-
555	3	Strong	-	Weak	-
595	12	Medium	Medium	Faint	Trace
(b) Specimens containing 42% Mg.					
505	1	Strong	Faint	Faint	-
555	3	Weak	-	Medium	-
595	12	-	-	Strong	-

percentages of this light metal present and by the lower scattering power of the magnesium atom as compared with the copper atom.

In these systems the tendency towards the formation of a compound having a structure similar to that of $CuAl_2$ would appear to be greater than that towards the formation of a high melting compound with a simple structure. The fact that in these systems the electrochemical factor is relatively large may influence the choice of compound.

EXPERIMENTS INVOLVING THE DEPOSITION OF ONE METAL ON ANOTHER IN VACUUM.

In order to find what effects the experimental techniques used might have on the results obtained, it was decided to try a different method

of specimen preparation. The method chosen was that of evaporating aluminium under low pressure and depositing it onto the surface of another metal. The copper-aluminium system was chosen for those experiments, the aluminium being deposited onto a thin copper compact previously heated to a constant temperature. Because of the relative proportions of copper and aluminium the overall composition of the deposited compact was always still in the α solid solution range.

TABLE XVI.

Structures obtained by Vaporising Aluminium onto Copper at various Temperatures.

Temp. °C.	Copper	Copper S.S.	Cu_9Al_4	$CuAl_2$	Al
40	V.strong	Faint	-	-	Weak
60	V.strong	Faint	-	-	Weak
80	V.strong	Faint	-	-	Weak
100	V.strong	Faint	-	-	Weak
170	V.strong	Faint	-	Trace	Weak
215	V.strong	Faint	V.weak	Weak	V.weak
270	V.strong	Faint	V.weak	Weak	Faint
385	V.strong	Weak	Weak	Faint	Faint
540	Strong	Strong	V.weak	V.weak	Faint.

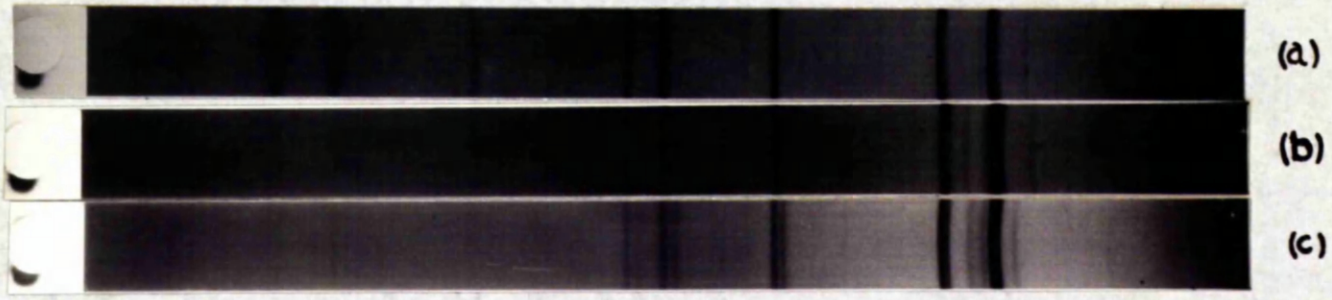

FIG. 19; X-RAY PHOTOGRAPHS OF SPECIMENS PREPARED BY DEPOSITING ALUMINIUM VAPOUR ONTO COPPER TARGETS HEATED TO VARIOUS TEMPERATURES.

a), TARGET AT 40°C.
b), TARGET AT 270°C.
c), TARGET AT 540°C.

Table XVI comprises the data relating to the structures which were present. It will be seen that $CuAl_2$ is first observed in a compact heated to a temperature as low as 170°C. This temperature is considerably lower than the temperature at which the compound forms in either the differential thermal or long time annealing experiments.

It will be observed from Fig.19 that though the lines due to copper are broad, all other lines are fine. This could be due to the fact that the film of aluminium or compound is very thin while the block of copper on which it lies is comparatively large. There is more scattered radiation with these specimens than with powder packed in vitreosil tubes. This would appear to be due to the larger bulky specimen and possibly also to the very fine or micro-crystalline nature of the deposited film. When aluminium was deposited onto a block of rock salt heated to 40°C, the structure of the metal film appeared to be almost amorphous(47). After aging at room temperature for 60 hours, the structure became much more crystalline. There was also evidence at this time of some orientation of the metal grains.

As can be seen from Fig. 19 , when the target temperature is 540°C the X-ray photograph shows two strong cubic patterns. It will be seen that the corresponding lines from each series are arranged in pairs, the distance between the two lines in a pair increasing towards the high angles. The higher angle line of each pair, corresponds to a pure copper line. The remaining lines, each of which is of almost equal intensity to the corresponding copper line, have a face centred cubic lattice with parameter $a = 3.660\text{Å}$. This is in good agreement the value (3.664Å) given by

Bradley and Jones(30) for a saturated solid solution of aluminium in copper. The most feasible explanation would seem to be that the copper compact is covered with a film of α solid-solution of the limiting composition. In addition to these lines belonging to a copper lattice, there are lines of a lower intensity corresponding to $CuAl_2$ and Cu_9Al_4.

At target temperatures lower than 540°C lines corresponding to the solid solution are of a lower intensity, but one line, corresponding to the strongest line of the series can be seen, even in the specimen taken from a target heated to 40°C. It would appear, therefore, that a very thin film of α solid solution can form before compound formation takes place. The fact that aluminium atoms can enter the copper lattice at temperatures as low as 40°C is an indication of their high mobility during condensation of the vapour.

As has been said already the first evidence of the formation of $CuAl_2$ is found with the target at a temperature of 170°C. Further increase of the temperature of the target gives lines characteristic of Cu_9Al_4 accompanied by a decrease in intensity of the lines corresponding to $CuAl_2$. At a target temperature of 540°C, in addition to the copper lines which are common to all specimens, the strongest lines are those of the α solid solution, with small quantities of the other compounds.

An investigation was also made of the changes in structure occurring when a film, deposited on cold copper, is heated to various constant temperatures for one hour. After furnace cooling, X-ray photographs were taken, and the specimens found to have the structures shown in Table XVII. Fig. 20 shows some of the X-ray photographs used to determine the structures, and

FIG. 20; X-RAY PHOTOGRAPHS OF SPECIMENS PREPARED BY DEPOSITING ALUMINIUM VAPOUR ONTO COPPER TARGETS AT ROOM TEMPERATURE AND SUBSEQUENTLY ANNEALING THEM FOR ONE HOUR.

a), ANNEALED AT 100°C.
b), ANNEALED AT 200°C.
c), ANNEALED AT 400°C.
d), ANNEALED AT 600°C.

illustrates the changes taking place.

TABLE XVII.

Structures Obtained in an Evaporated Film after 1 hour at Various Temperatures.

Temp. °C.	Copper	Cu.S.S.	Cu_9Al_4	$CuAl_2$	Aluminium
As deposited	V.Strong	Faint	-	-	Weak
100	V.Strong	V.Weak	-	-	Weak
200	V.Strong	V.Weak	-	-	Weak
300	V.Strong	Weak	-	-	Weak
400	V.Strong	Weak	-	V.Weak	V.Weak
500	V.Strong	Weak	Faint	Faint	V.Weak
600	Strong	Strong	V.Weak	-	-

It will be seen that no lines corresponding to $CuAl_2$ are detected until 400°C. As the annealing temperature is raised further the intensity of the $CuAl_2$ lines decrease and lines appear which correspond to Cu_9Al_4. At an annealing temperature of 600°C. the lines corresponding to $CuAl_2$ and Cu_9Al_4 are of low intensity while those corresponding to the α solid solution are strong. The structure is believed to be almost exactly the same as that obtained by depositing aluminium onto a copper target at 540°C.

FIG. 21; PHOTOMICROGRAPH OF ALUMINIUM DEPOSITED ONTO A COPPER TARGET HEATED TO 385°C. UNETCHED. x 1100.

It will be seen that the lowest temperature at which compound formation is observed is of the same order as that at which it is first observed in annealed powder compacts. The time required, however, has been very much reduced.

It may be mentioned here that, under conditions similar to this last investigation, Takahashi and Trillat(48) have also found $CuAl_2$ to be the first compound to form.

Metallographic sections have been made from some of the copper compacts on which aluminium has been deposited. A typical section is shown in Fig. 21 which is the cross-section of a compact heated to 385°C before the deposition of aluminium vapour. The white film seen on the surface of the copper contains, according to X-ray data, aluminium, $CuAl_2$ and Cu_9Al_4. It will be seen how it has followed the contours of the copper surface exactly and penetrated into comparatively deep pores.

This specimen was examined under polarised light. Partial extinction was observed in a narrow band of the deposited layer, next to the copper. The band appeared to vary between being almost extinct and very slightly extinct. No definite grains were seen, and it is thought that the film was composed of randomly orientated micro crystals so preventing complete extinction from being observed. Due to the diffuse appearance of this narrow band, it was not possible to photograph it under polarised light.

It would appear, therefore, that by the use of vacuum deposition techniques compound formation can occur at much lower temperatures and in much shorter times than has been observed in either of the methods involving

the use of compressed powders.

It was not possible to undertake a complete survey of the reactions occurring in the iron-aluminium system, using this technique, but initial results have shown that if the temperature of the iron target is below 250°C no reaction will take place during the time of deposition. However, when the temperature of the target was raised to 350°C it was found that the lines corresponding to aluminium have been replaced by those of Fe_3Al_8 although of weak intensity. It should be noted that no $FeAl_6$ was present in this specimen. The colour of the deposited film also underwent a change, being silver grey when composed of aluminium and dark grey after compound formation had occurred.

It would thus appear that the reactions taking place here, are again similar to those in annealed compacts made from mixed powders, the only differences seeming to be in the rates of reaction.

The method of specimen preparation and the means of following the course of the reaction do not, therefore, appear to affect the reaction taking place, though they may affect the speed of the reaction.

CHAPTER V.

DISCUSSION OF RESULTS.

TABLE XVIII.

	Observed Results.				Data Relating to Phase First Formed.					
Compound	Reaction Temp. °C.	Heat Evolution °C.	Reaction Tr MP of phase °K/°K.	Congruent M.P.	Highest M.P. of system.	Crystal structure	$-\Delta H$ kcal/mol.	Highest ΔH of system	e/a	Electrochemical Factor for System.
Fe_2Al_5	570	575	0.58	Yes	Near	Orthorhombic.	47	Yes	2.15	1.23
$NiMg_2$	440	43	0.68	No	No	Hex	22.6	Yes	1.33	1.32
Ni_5Zn_{21}	300	346	0.50	Yes	No	Cubic (γ brass)	49 ($NiZn_{4.2}$)	Yes	1.61	0.53
NiAl	550 694	75 700	0.43 0.51	Yes	Yes	B.C.C.	34	Near	1.5	1.05
$CuMg_2$	480	25	0.90	Yes	No	Orthorhombic.	23.5	Near	1.67	1.89
CuZn	210	45	0.41	No	Yes	B.C.C.	18	No	1.5	1.10
$CuAl_2$	450	112	0.76	No	No	Body-centred tetrag.	9.5	No	2.33	1.62

DISCUSSION OF RESULTS.

The results obtained in the various systems investigated have been summarised in Table XVIII which also contains some data relating to the phases formed.

It can be seen that a correlation exists between the heat evolution and the heat of formation of the compound. When the heat of formation is low as in the case of CuZn, the heat evolution is also low. Conversely when the heat of formation is high the observed heat change is high (as in NiAl). Very often the compound formed is that with the highest heat of formation in the system. Similarly in the majority of cases the compound formed has a congruent melting point and is stable to a higher temperature than any of the other intermediate phases in the system. However, all of these conditions may not be satisfied in the same system.

It is interesting to note that in many cases the temperature at which the reaction occurs is approximately half the melting temperature of the compound formed. If the value for $CuMg_2$ be disregarded the average reaction temperature is 0.56 of the melting temperature. It has been observed by Oriani(49) that for many alloys the temperature of ordering is 0.63 or 0.55 of the solidus temperature of the alloy, depending whether it is a 1:1 or 1:3 alloy. Since ordering represents the formation of a compound from a random mixture of atoms, there may well be some significance in agreement between the observed reaction temperature and the temperature of ordering.

It will be seen that most of the compounds have fairly low electron concentrations. Thus two compounds have a ratio of 21/13 and two more a ratio of 3/2 while only two, $CuAl_2$ and Fe_2Al_5 have ratios in excess of 2.; assuming iron to have zero valency.

The structures of the compounds formed seem to divide into two classes, body centred cubic or γ brass, and a complex structure which is related in some way to the $CuAl_2$ structure. It will be observed that the structures of high symmetry occur in systems of low electrochemical factor while the complex structures occur in systems of high electrochemical factor. This may have some bearing on the fact that in the nickel-aluminium system, NiAl is formed and not $NiAl_3$ as one might have expected by analogy with the other aluminium systems.

A point of interest arises from the copper-aluminium results. The lowest temperature at which compound formation was detected during the deposition of aluminium onto copper was 170°C which is the same as the initial temperature at which Hoyat, Craik and Cranston(16) detected compound formation in the copper-zinc system, while studying the sintering of pressed compacts by X-ray techniques. In both cases a vapour is in contact with a copper surface so that an agreement in reaction temperature is not unexpected.

It has been mentioned already in connection with the vacuum deposition experiments that there appeared to be a very faint film of copper solid solution even in compacts exposed to aluminium vapour at room temperature. This would seem to indicate a very high mobility of the aluminium atoms and of the surface copper atoms. As has been

suggested in a number of papers presented recently at a Symposium on powder metallurgy(50) a high mobility of surface atoms can be a very powerful factor in accelerating sintering reactions in metal compacts.

The method of compound formation when aluminium is deposited onto copper at an elevated temperature may be that aluminium diffuses into the copper lattice until the surface layers reach the composition of $CuAl_2$ when, provided the temperature is high enough the exothermic reaction can commence. At room temperature only a few aluminium atoms can enter the copper lattice to form a solid solution while most must deposit <u>on</u> the surface.

From this one might predict that in any of the other systems, or in copper-aluminium under normal annealing conditions, where the vapour phase is absent, a similar process might occur through surface diffusion bringing the two metals intimately together and volume diffusion over extremely short distances allowing the exothermic reaction to commence. Thereafter one or other metal must diffuse through the layer of compound already formed before further reaction can take place.

Since it is very possible that for many compounds the rate of diffusion of one constituent element through it is of the same order at the same fraction of the melting point of the compound, the fact that the reaction temperature was approximately half the melting temperature of the compound formed may be explained. As the melting point of a compound increases it is to be expected that the strength of the inter-atomic bonding will increase. With stronger interatomic bonding the rate of diffusion of one of the constituent elements through the

compound may be lower than it would be through another lower melting compound in the system at the same temperature. This would tend to favour the formation and growth of the lower melting compound.

It is possible that the activation energy necessary to form a compound from its elements varies between different compounds in any system, and if this be so then the most stable compound may be formed in a reaction requiring an activation energy which is considerably greater than that necessary to form another less stable compound. If there are two compounds, each of which is of reasonable stability but one of which, the more stable, requires a higher activation energy, then the less stable compound will be formed. However, the more stable compound may subsequently be enabled to form by the heat evolved in the initial reaction. This would explain why a compound of comparatively low melting point, low heat of formation and complex structure may form in certain systems. In these systems as has been said the electro-chemical factor is high so that in the complex structures it is to be expected that there will be some degree of covalent bonding. This will probably result in these compounds requiring a lower activation energy than others with a true metallic lattice of high symmetry.

It will be remembered that in the copper-aluminium system Cu_9Al_4 forms at an early stage in the reactions and persists during most of the sintering process. It had been thought possible from a consider-ation of the copper-zinc and nickel-zinc results and from a study of the copper-aluminium diagram that this compound might well be the first to form, as its stability appeared to be high. The reason why $CuAl_2$,

which appears to be less stable, forms first may be that the activation energy required is less than for the formation of Cu_9Al_4. If this be so it might be expected that Cu_9Al_4 would be enabled to form by the heat evolved during the initial reaction or by raising the annealing temperature slightly. Due to its high melting point the rate of diffusion of aluminium through it may be comparatively low which, along with its stability, would account for its persistence in non-equilibrium conditions even after long annealing times at fairly high temperatures.

During this investigation several observations have been made about the experimental methods used. It has been seen that in any system the magnitude of the exothermic change observed in differential thermal analysis rises to a maximum at one composition. With the exception of the copper-aluminium system this maximum occurs at the composition of the compound which forms first, as confirmed by X-ray investigation.

In the case of the copper-aluminium system is has been suggested that the formation of a liquid phase, which can occur at about the temperature of the reaction, may affect the observed magnitude of the reaction. In the copper-magnesium system a liquid phase is found at a temperature very near to that at which the heat change occurs in differential thermal analysis. In this system, however, the exothermic reaction is small and the temperature of the specimen does not rise high enough for liquid phase formation to interfere.

As can be seen by the graphs such as that in Fig. 18 , the magnitude of the exothermic reaction appears to vary uniformly with change in composition. If the graphs be extrapolated till the magnitude is zero, it can be seen that the composition at which this occurs varies from zero for iron-aluminium to 20 at. percent for copper-aluminium. X-ray data have shown that the quantities of the two metals remaining after an exothermic reaction vary from system to system. In some systems none can be observed while in others comparatively large quantities can be observed.

Obviously it would be of considerable value to be able to calculate in any given compact the quantity of compound formed during the exothermic change. This has been done for a number of iron-aluminium specimens.

The main difficulty in the calculation is that during the exothermic change the compact is losing heat by radiation and conduction. Thus the observed maximum in the differential thermocouple is not a true maximum, though it is quite suitable for comparison with other specimens.

One of the graphs obtained, that for a 54% Al compact, is shown in Fig. 22 . Applying Newton's law of cooling, the section of the curve CD may be accurately predicted. It is not possible, however, to apply this law to the portion B.C. As the temperature of the specimen is continuously rising, due to what is in effect a continuous heat input, it would be necessary to divide this portion for the purposes of calculation into many steps of instantaneous heat input,

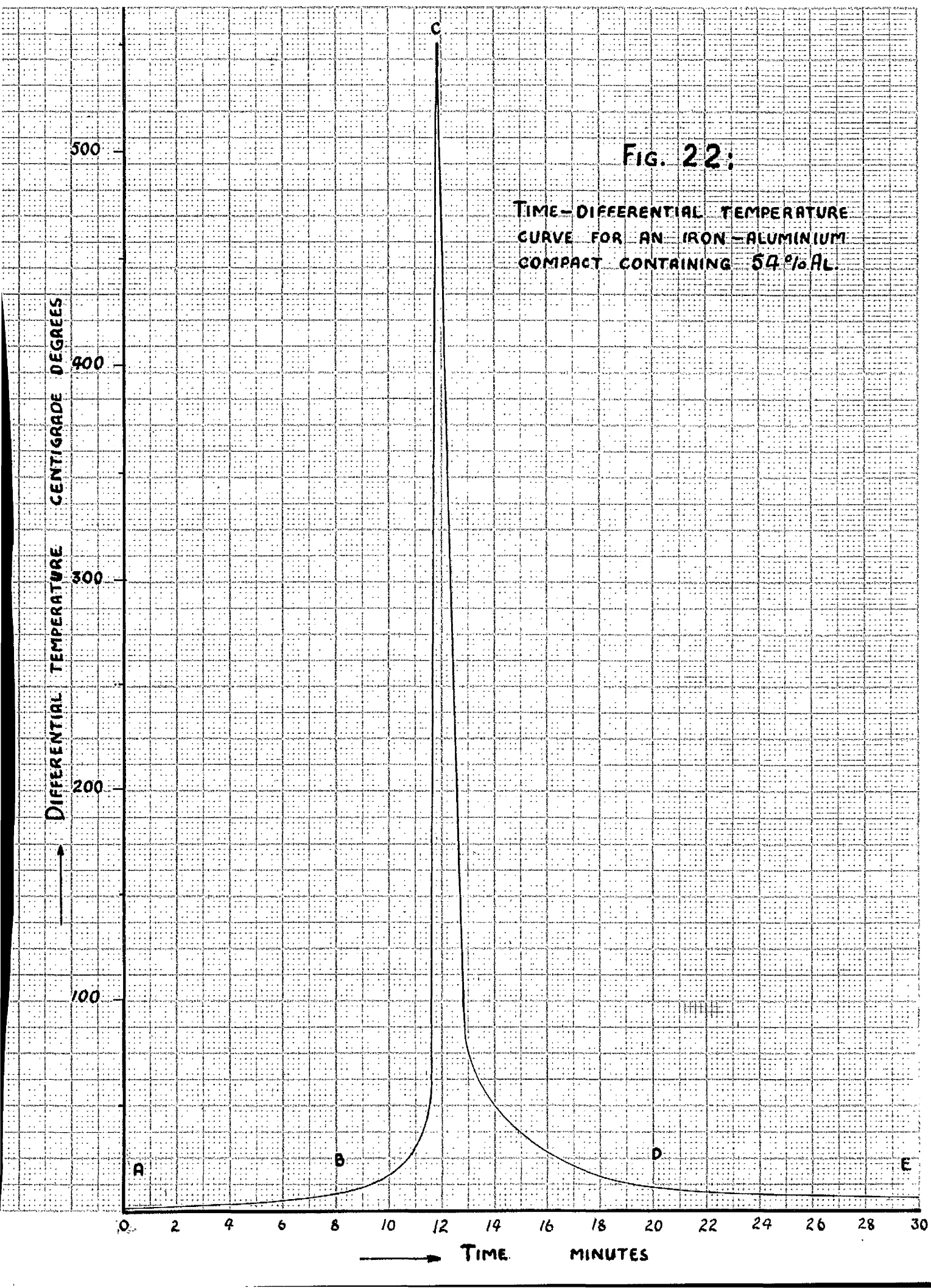

FIG. 22;

TIME-DIFFERENTIAL TEMPERATURE CURVE FOR AN IRON-ALUMINIUM COMPACT CONTAINING 54% AL.

so enabling Newton's law to be applied. Owing to the experimental difficulties involved, there are insufficient observed points on this portion of the curve to allow this to be done. It has been necessary, therefore, to use a more empirical method of calculating the heat loss over the portion B.C. of the curve.

It has been assumed that at any temperature the rate of heat loss is the same, whether the temperature of the specimen be rising or falling. Thus the average rate of heat loss when the temperature of the specimen rises through a given interval will be the same as when the temperature falls through the same interval.

From the time taken for the specimen to cool from C to D an average rate of cooling can be derived. Using this value and the time taken for the temperature of the specimen to rise from B to C, it is possible to calculate the theoretical temperature which would have been attained in the absence of any cooling losses. Using this theoretical maximum temperature the quantity of heat evolved as a result of the reaction can be calculated in the normal manner.

The maximum quantity of heat which can be liberated in any specimen can be found by multiplying the heat of formation by the mole fraction of the compound which is thought to be present. If one element is present in a smaller amount than in the compound, then the whole weight of this metal is considered to react with some of the other to form a smaller weight of compound. This weight of compound is then used to find the molefraction which theoretically may be formed.

Since no published value for the heat of formation of Fe_2Al_5 could be found, an approximation was calculated using Neumann and Kopp's rule. The application of the rule to the iron-aluminium system was checked by calculating the molar heats of $FeAl_2$ and $FeAl_3$. Values in good agreement with the published values were obtained. The value calculated for Fe_2Al_5 was 47 k.cals/mol.

The quantity of heat evolved in a 54% Al specimen, (i.e., at the composition of Fe_2Al_5) after allowing for cooling losses is 96% of that theoretically possible, indicating that the reaction has been almost complete. An X-ray photograph of this specimen showed no iron or aluminium lines, so confirming the calculated result.

TABLE XIX.

Calculation of the amount of compound formation possible in various iron-aluminium alloys.

Composition		Specimen Weight	Theoretical Compound Wt.	Max. Temp. (No heat loss)	Calculated heat evolution cals.	Theoretically possible H.E. cals.	Ratio
Fe	Al	gms.	gms.	°C.			%
68	32	19.597	11.620	513	2,205	2,215	99
51	49	7.0073	6.341	665	1,110	1,204	92.5
46	54	7.3662	7.3662	750	1,348	1,400	96
42	58	7.0600	6.441	700	1,227	1,229	100

The various steps in the calculation of the percentage reaction are shown in Table XIX along with the corresponding figures for other compositions, namely 32%, 49%, and 58% Al. These compositions lie on either side of the composition of Fe_2Al_5, the first two having excess iron, the others excess aluminium. It will be seen from the Table that Fe_2Al_5 formation is almost complete as far as stoichiometric proportions permit. As a result of this it would be expected that the heat evolution should vary regularly with the composition of the compact and reach a maximum at the composition of the compound being formed. It would appear, therefore, that one is justified in accepting the results of the various graphs of magnitude of reaction against composition.

Mention was made earlier of the speed of the reaction during deposition of aluminium onto copper. In the system copper-aluminium for identical compacts the temperature of compound formation can be lowered by lengthy annealing. Thus differential thermal analysis indicates that the reaction is most rapid at 460°C, but by annealing a similar compact at 400°C for 2½ days compound formation can be detected. However, by depositing aluminium vapour onto a copper compact heated to 170°C, appreciable compound formation can be detected after ½ minute.

It has already been mentioned that this is due in part to the increased mobility of the aluminium atoms. Treatment of the copper compact by hydrogen immediately prior to deposition of aluminium would remove any adsorbed, or combined layer of oxygen and probably

further increase the mobility of the copper atoms, so possibly lowering the temperature of the initial reaction still further.

If, after depositing aluminium onto a copper compact at room temperature, the whole be annealed, compound formation can be detected after 1 hour at 400°C. The great reduction in time compared with the normal compact is due to the increased contact area between the aluminium and copper and to the absence of a surface film of oxide on the aluminium particles.

CHAPTER VI.

GENERAL SUMMATION AND CONCLUSIONS.

GENERAL SUMMATION AND CONCLUSIONS.

It has been shown that differential thermal analysis is a reliable method of investigating any possible compound formation in an intermetallic system, provided that any exothermic reaction occurring does not carry the compact temperature above the liquidus of the system.

X-ray analysis is required to identify the particular compound formed by the exothermic reaction. For this purpose specimens may be prepared by annealing at elevated temperatures or by depositing one metal onto the surface of the other, at elevated temperatures. This latter method may in some cases yield more definite information than the more usual annealing method, as happened in the iron-aluminium system.

It is not possible at this stage to forecast conclusively exactly which compound will form first in any given system. In general it will be the compound with the highest stability which will usually be indicated by a high, congruent melting point, a high heat of formation and a simple crystal structure of high symmetry.

However, in certain systems there may be another compound, which, though it is of lower stability, requires a lower activation energy for its formation. In this case the most stable compound will not be formed first though it may appear during the sintering reactions and subsequently remain in non-equilibrium conditions for long periods of time.

REFERENCES.

1. Roberts, J.P. Metallurgia, 1950, vol.42, No.250, p.123.

2. Goetzel, C.G. Treatise on Powder Metallurgy, Vol.II, 1950, Interscience Publishers Inc., N.Y.

3. Kuczynski, G.C. J. of Metals, 1949, Vol.1, p.169.

4. Cabrera, N. Trans. A.I.M.E., 1950, Vol.188, p.667.

5. Arthur, G. J.Inst.Metals, 1954-55, Vol.83 (7), p.329.

6. Frenkel, J. J.Phys. (U.S.S.R.) 1945, vol.9, p.385.

7. Clark, P.W. and White, J. Trans.Brit.Ceramic Soc., 1950, Vol.49, p.305.

8. Smigelskas, A.D. and Kirkendall, E.O. Trans. A.I.M.E., 1947, Vol.171, p.130.

9. da Silva, L.C.C. and Mehl, R.F. J. of Metals, 1951, Vol.3, p.155.

10. Barnes, R.S. Proc.Phys.Soc., 1952, (B), vol.65, p.512.

11. Le Claire A.D., and Barnes, R.S. J. of Metals, 1951, Vol.3, p.1060.

12. Butler, J.M. and Hoare, T.P. J.Inst.Metals, 1951-52, Vol.80, p.207.

13. Raub, E. and Plate, W. Zeit.Metallkunde, 1951, Vol.42, p.76.

14. Duwez, P. and Jordan, C.B. "The Physics of Powder Metallurgy" p.280, 1951, McGraw Hill Book Co.,N.Y.

15. Duwez, P. International Symposium on Powder Metallurgy, Graz. 1948. Reported in Metal Industry 1948, Vol.73 (7), p.129.

16. Howat, D.D., Craik, R.L. and Cranston, J.P. J. Inst.Metals, 1951-52, Vol.80, p.353.

17. Cranston, J.P. Ph.D.Thesis, 1951, University of Glasgow.

18. Mott B.W., and Haines, H.R., J.Inst.Metals, 1951-52, Vol.80, p.629.

19. Rhines F.N., and Colton R.A. Symposium on Powder Metallurgy, p.67, 1942, A.S.M.Cleveland, Ohio.

20. Michel P. Compt. Rend. 1953, Vol.237 (4), p.332.

21. Michel P. Compt. Rend. 1952, Vol.235 (5), p.377.

22. Goldsztaub S. and Michel P., Compt.Rend. 1951, Vol.232 (20), p.1843.

23. Michel P. Compt. Rend., 1953, Vol.236 (8), p.820.

24. Takahashi N, and Trillat, J.J. Métaux 1953, No.339, p.185.

25. Nelson, J.B., and Riley D.P. Proc. Phys.Soc., 1945,(A), Vol.57, p.160.

26. Phillips, A. and Brick R.M. Metals Handbook, p.1206, 1948, A.S.M. Cleveland, Ohio.

27. Lacey, C.E. Metals Handbook, p.1236, 1948, A.S.M.Cleveland, Ohio.

28. Fink, W.L., Willey L.A., and Smith C.S., Metals Handbook, p.1159, 1948, A.S.M. Cleveland, Ohio.

29. Wassermann, G. Metallwirtschaft, 1934, Vol.8, p.133.

30. Bradley, A.J., and Jones P. J.Inst.Metals, 1933, Vol.51, p.131.

31. Isaitschew, I, Kaminsky, E, and Kurdjumow G. Trans. A.I.M.E., 1938, Vol.128, p.361.

32. Gawranek, V, Kaminsky E, and Kurdjumow G. Metallwirtschaft, 1936, Vol.15, p.370.

33. Greninger A.B., Trans. A.I.M.E., 1939, Vol.133, p.204.

34. Taylor, A. "An Introduction to X-ray Metallography" p.369, 1949, Chapman and Hall, London.

35. Fink, W.L. and Willey L.A. Metals Handbook, p.1161, 1948. A.S.M. Cleveland, Ohio.

36. Taylor, A. "An Introduction to X-ray Metallography" p.366, 1949, Chapman and Hall, London.

37. Schubert, K. and Kluge, M. Z.Naturforsch, 1953, Vol.8a, p.755.

38. Hume-Rothery, W, and Coles B.R. Advances in Physics, 1954, Vol.3, (10), p.149.

39. Schubert, K, Rösler U, Kluge M, Anderko K, Härle L. Naturwiss, 1953, Vol.40, p.437.

40. Bachmetew, E. Z.Krist. 1934, Vol.88, p.179.

41. Black, P.J. Acta.Cryst., 1955, Vol.8, p.43.

42. Fink, W.L. and Willey, L.A. Metals Handbook, p.1164, 1948, A.S.M. Cleveland, Ohio.

43. Craik, R.L., Ph.D., Thesis, 1952, University of Glasgow.

44. Hall, A.M. Metals Handbook, p.1225, 1948, A.S.M. Cleveland, Ohio.

45. Sagor, G.F., Nelson, B.J., Metals Handbook, p.1197, 1948, A.S.M. Cleveland, Ohio.

46. Schubert K. and Kluge, M.S., Z.Metallkunde, 1951, Vol.42, p.321.

47. Wylie, T.S. Met.Phil.Dept., Royal Technical College, Glasgow, Private Communication.

48. Takahashi, N. and Trillat, J.J. Acta.Met. 1954, Vol.2 (3), p.409.

49. Oriani, R.A. Acta. Met. 1954, Vol.2 (2), p.343.

50. Symposium on Powder Metallurgy, 1954, Iron and Steel Inst., London.

A C K N O W L E D G M E N T S.

The author wishes to express his thanks to Professor Hay and to Dr. D.D.Howat for their continued and valuable interest, advice and criticism during the course of this work.

The interest of Mr. T.S. Wylie of the Natural Philosophy Department, of the Royal Technical College, in certain sections of this work and his criticism of these sections is gratefully acknowledged.

The work was carried out in the Metallurgy Department of the Royal Technical College, Glasgow.